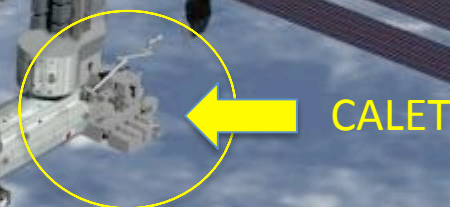


# CALET: Calorimetric Electron Telescope

Vulcano Workshop 2018, May 22

Pier Simone Marrocchesi  
University of Siena & INFN-Pisa  
for the CALET Collaboration





# CALET collaboration team



O. Adriani<sup>25</sup>, Y. Akaike<sup>2</sup>, K. Asano<sup>7</sup>, Y. Asaoka<sup>9,31</sup>, M.G. Bagliesi<sup>29</sup>, G. Bigongiari<sup>29</sup>, W.R. Binns<sup>32</sup>, S. Bonechi<sup>29</sup>, M. Bongi<sup>25</sup>, P. Brogi<sup>29</sup>, J.H. Buckley<sup>32</sup>, N. Cannady<sup>12</sup>, G. Castellini<sup>25</sup>, C. Checchia<sup>26</sup>, M.L. Cherry<sup>12</sup>, G. Collazuol<sup>26</sup>, V. Di Felice<sup>28</sup>, K. Ebisawa<sup>8</sup>, H. Fuke<sup>8</sup>, G.A. de Nolfo<sup>14</sup>, T.G. Guzik<sup>12</sup>, T. Hams<sup>3</sup>, M. Hareyama<sup>23</sup>, N. Hasebe<sup>31</sup>, K. Hibino<sup>10</sup>, M. Ichimura<sup>4</sup>, K. Ioka<sup>34</sup>, W. Ishizaki<sup>7</sup>, M.H. Israel<sup>32</sup>, A. Javid<sup>12</sup>, K. Kasahara<sup>31</sup>, J. Kataoka<sup>31</sup>, R. Kataoka<sup>16</sup>, Y. Katayose<sup>33</sup>, C. Kato<sup>22</sup>, Y. Kawakubo<sup>1</sup>, N. Kawanaka<sup>30</sup>, H. Kitamura<sup>15</sup>, H.S. Krawczynski<sup>32</sup>, J.F. Krizmanic<sup>2</sup>, S. Kuramata<sup>4</sup>, T. Lomtadze<sup>27</sup>, P. Maestro<sup>29</sup>, P.S. Marrocchesi<sup>29</sup>, A.M. Messineo<sup>27</sup>, J.W. Mitchell<sup>14</sup>, S. Miyake<sup>5</sup>, K. Mizutani<sup>20</sup>, A.A. Moiseev<sup>3</sup>, K. Mori<sup>9,31</sup>, M. Mori<sup>19</sup>, N. Mori<sup>25</sup>, H.M. Motz<sup>31</sup>, K. Munakata<sup>22</sup>, H. Murakami<sup>31</sup>, Y.E. Nakagawa<sup>8</sup>, S. Nakahira<sup>9</sup>, J. Nishimura<sup>8</sup>, S. Okuno<sup>10</sup>, J.F. Ormes<sup>24</sup>, S. Ozawa<sup>31</sup>, L. Pacini<sup>25</sup>, F. Palma<sup>28</sup>, P. Papini<sup>25</sup>, A.V. Penacchioni<sup>29</sup>, B.F. Rauch<sup>32</sup>, S.B. Ricciarini<sup>25</sup>, K. Sakai<sup>3</sup>, T. Sakamoto<sup>1</sup>, M. Sasaki<sup>3</sup>, Y. Shimizu<sup>10</sup>, A. Shiomi<sup>17</sup>, R. Sparvoli<sup>28</sup>, P. Spillantini<sup>25</sup>, F. Stolzi<sup>29</sup>, I. Takahashi<sup>11</sup>, M. Takayanagi<sup>8</sup>, M. Takita<sup>7</sup>, T. Tamura<sup>10</sup>, N. Tateyama<sup>10</sup>, T. Terasawa<sup>7</sup>, H. Tomida<sup>8</sup>, S. Torii<sup>9,31</sup>, Y. Tunesada<sup>18</sup>, Y. Uchihori<sup>15</sup>, S. Ueno<sup>8</sup>, E. Vannuccini<sup>25</sup>, J.P. Wefel<sup>12</sup>, K. Yamaoka<sup>13</sup>, S. Yanagita<sup>6</sup>, A. Yoshida<sup>1</sup>, K. Yoshida<sup>21</sup>, and T. Yuda<sup>7</sup>

- 1) Aoyama Gakuin University, Japan
- 2) CRESST/NASA/GSFC and Universities Space Research Association, USA
- 3) CRESST/NASA/GSFC and University of Maryland, USA
- 4) Hirosaki University, Japan
- 5) Ibaraki National College of Technology, Japan
- 6) Ibaraki University, Japan
- 7) ICRR, University of Tokyo, Japan
- 8) ISAS/JAXA Japan
- 9) JAXA, Japan
- 10) Kanagawa University, Japan
- 11) Kavli IPMU, University of Tokyo, Japan
- 12) Louisiana State University, USA
- 13) Nagoya University, Japan
- 14) NASA/GSFC, USA
- 15) National Inst. of Radiological Sciences, Japan
- 16) National Institute of Polar Research, Japan
- 17) Nihon University, Japan

- 18) Osaka City University, Japan
- 19) Ritsumeikan University, Japan
- 20) Saitama University, Japan
- 21) Shibaura Institute of Technology, Japan
- 22) Shinshu University, Japan
- 23) St. Marianna University School of Medicine, Japan
- 24) University of Denver, USA
- 25) University of Florence, IFAC (CNR) and INFN, Italy
- 26) University of Padova and INFN, Italy
- 27) University of Pisa and INFN, Italy
- 28) University of Rome Tor Vergata and INFN, Italy
- 29) University of Siena and INFN, Italy
- 30) University of Tokyo, Japan
- 31) Waseda University, Japan
- 32) Washington University-St. Louis, USA
- 33) Yokohama National University, Japan
- 34) Yukawa Institute for Theoretical Physics, Kyoto University, Japan



# CALET collaboration team

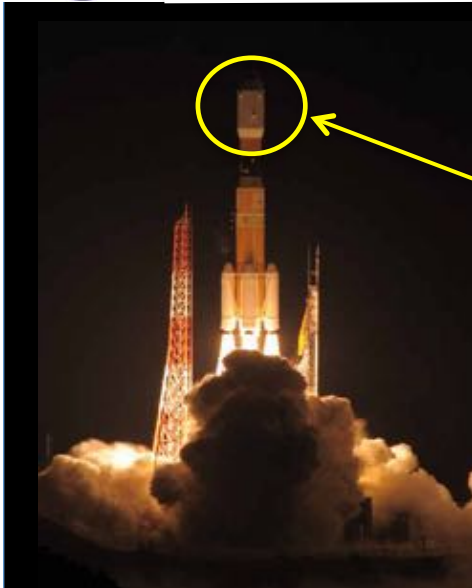
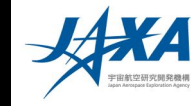


O. Adriani<sup>25</sup>, Y. Akaike<sup>2</sup>, K. Asano<sup>7</sup>, Y. Asaoka<sup>9,31</sup>, M.G. Bagliesi<sup>29</sup>, G. Bigongiari<sup>29</sup>, W.R. Binns<sup>32</sup>, S. Bonechi<sup>29</sup>, M. Bongi<sup>25</sup>, P. Brogi<sup>29</sup>, J.H. Buckley<sup>32</sup>, N. Cannady<sup>12</sup>, G. Castellini<sup>25</sup>, C. Checchia<sup>26</sup>, M.L. Cherry<sup>12</sup>, G. Collazuol<sup>26</sup>, V. Di Felice<sup>28</sup>, K. Ebisawa<sup>8</sup>, H. Fuke<sup>8</sup>, G.A. de Nolfo<sup>14</sup>, T.G. Guzik<sup>12</sup>, T. Hams<sup>3</sup>, M. Hareyama<sup>23</sup>, N. Hasebe<sup>31</sup>, K. Hibino<sup>10</sup>, M. Ichimura<sup>4</sup>, K. Ioka<sup>34</sup>, W. Ishizaki<sup>7</sup>, M.H. Israel<sup>32</sup>, A. Javid<sup>12</sup>, K. Kasahara<sup>31</sup>, J. Kataoka<sup>31</sup>, R. Kataoka<sup>16</sup>, Y. Katayose<sup>33</sup>, C. Kato<sup>22</sup>, Y. Kawakubo<sup>1</sup>, N. Kawanaka<sup>30</sup>, H. Kitamura<sup>15</sup>, H.S. Krawczynski<sup>32</sup>, J.F. Krizmanic<sup>2</sup>, S. Kuramata<sup>4</sup>, T. Lomtadze<sup>27</sup>, P. Maestro<sup>29</sup>, P.S. Marrocchesi<sup>29</sup>, A.M. Messineo<sup>27</sup>, J.W. Mitchell<sup>14</sup>, S. Miyake<sup>5</sup>, K. Mizutani<sup>20</sup>, A.A. Moiseev<sup>3</sup>, K. Mori<sup>9,31</sup>, M. Mori<sup>19</sup>, N. Mori<sup>25</sup>, H.M. Motz<sup>31</sup>, K. Munakata<sup>22</sup>, H. Murakami<sup>31</sup>, Y.E. Nakagawa<sup>8</sup>, S. Nakahira<sup>9</sup>, J. Nishimura<sup>8</sup>, S. Okuno<sup>10</sup>, J.F. Ormes<sup>24</sup>, S. Ozawa<sup>31</sup>, L. Pacini<sup>25</sup>, F. Palma<sup>28</sup>, P. Papini<sup>25</sup>, A.V. Penacchioni<sup>29</sup>, B.F. Rauch<sup>32</sup>, S.B. Ricciarini<sup>25</sup>, K. Sakai<sup>3</sup>, T. Sakamoto<sup>1</sup>, M. Sasaki<sup>3</sup>, Y. Shimizu<sup>10</sup>, A. Shiomi<sup>17</sup>, R. Sparvoli<sup>28</sup>, P. Spillantini<sup>25</sup>, F. Stolzi<sup>29</sup>, I. Takahashi<sup>11</sup>, M. Takayanagi<sup>8</sup>, M. Takita<sup>7</sup>, T. Tamura<sup>10</sup>, N. Tateyama<sup>10</sup>, T. Terasawa<sup>7</sup>, H. Tomida<sup>8</sup>, S. Torii<sup>9,31</sup>, Y. Tunesada<sup>18</sup>, Y. Uchihori<sup>15</sup>, S. Ueno<sup>8</sup>, E. Vannuccini<sup>25</sup>, J.P. Wefel<sup>12</sup>, K. Yamaoka<sup>13</sup>, S. Yanagita<sup>6</sup>, A. Yoshida<sup>1</sup>, K. Yoshida<sup>21</sup>, and T. Yuda<sup>7</sup>





# CALET Payload

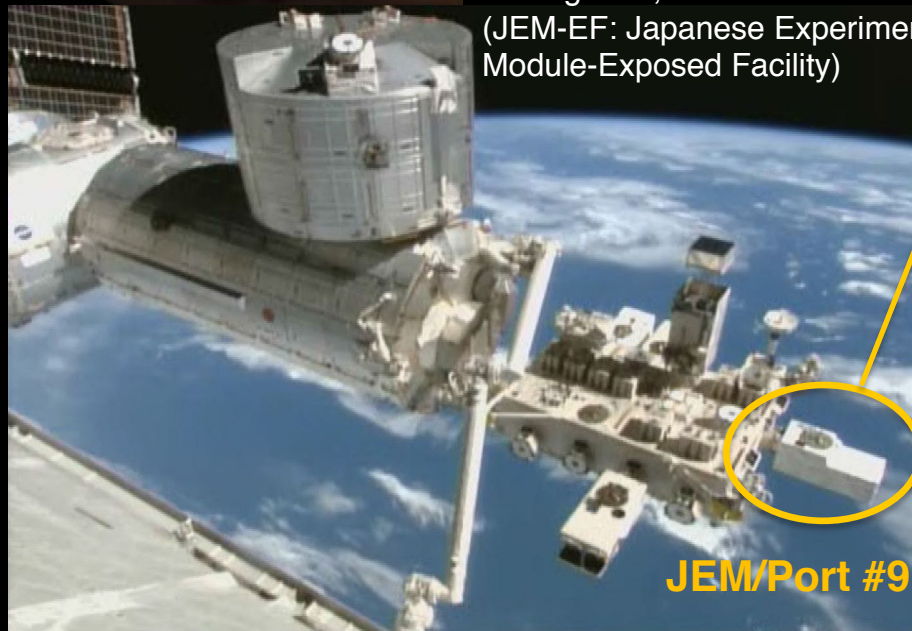


Kounotori (HTV) 5



Launched on Aug. 19<sup>th</sup>, 2015  
by the Japanese H2-B rocket

Emplaced on JEM-EF port #9  
on Aug. 25<sup>th</sup>, 2015  
(JEM-EF: Japanese Experiment  
Module-Exposed Facility)



JEM/Port #9

CGBM (CALET  
Gamma-ray  
Burst Monitor)

FRGF (Flight Releasable  
Grapple Fixture)

ASC (Advanced  
Stellar Compass)

Calorimeter

GPSR (GPS  
Receiver)

MDC (Mission  
Data Controller)

- **Mass:** 612.8 kg
- JEM Standard Payload **Size:**  
1850mm (L) × 800mm (W) × 1000mm (H)
- **Power Consumption:** 507 W (max)
- **Telemetry:**  
Medium 600 kbps (6.5GB/day) / Low 50 kbps

# ISS: a Cosmic Ray Observatory in Low Earth Orbit



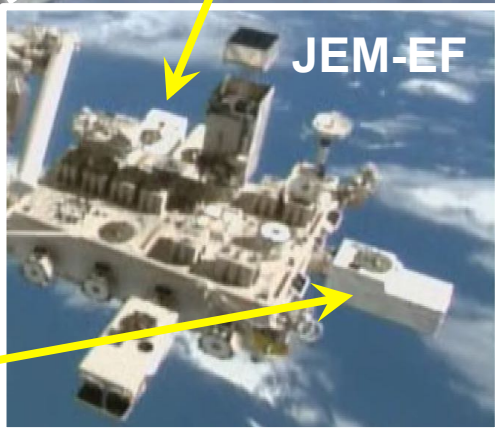
AMS Launch  
May 16, 2011



ISS-CREAM Launch  
August 14, 2017



CALET Launch  
August 19, 2015



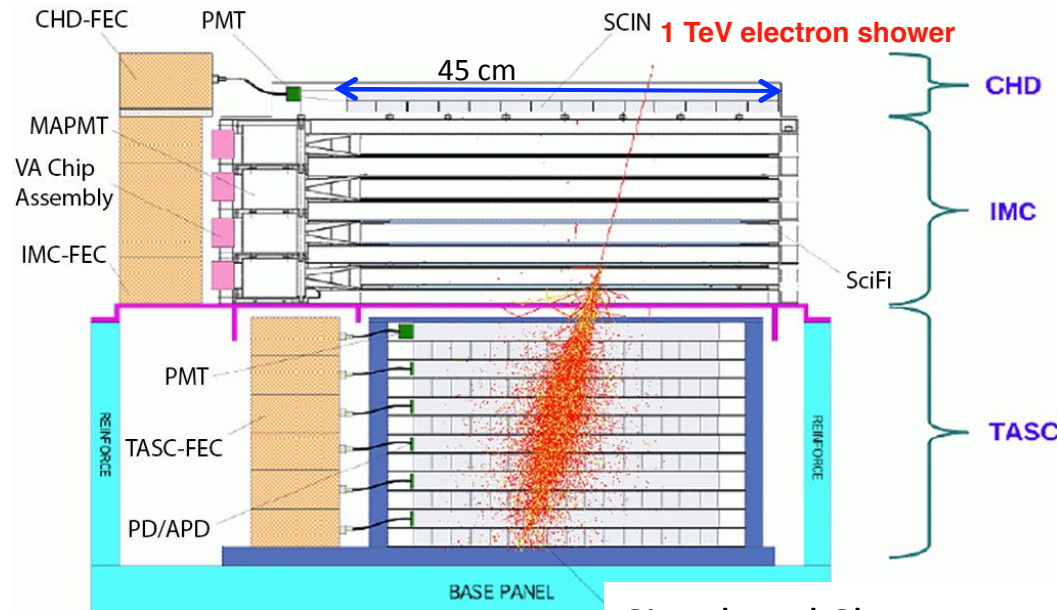
JEM-EF



# CALET Capability

Field of view:  $\sim 45$  degrees (from the zenith)

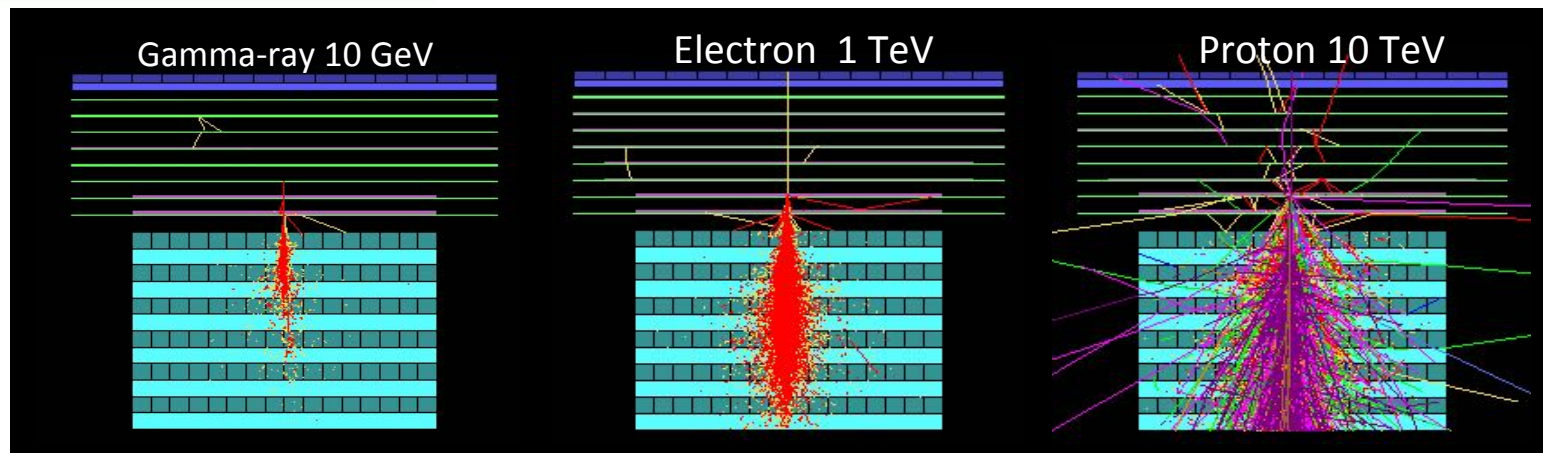
Geometrical Factor:  $\sim 1,040 \text{ cm}^2\text{sr}$  (for electrons)



## CALET: a unique set of key instruments

- ❑ **CHD**: a dedicated **charge detector + multiple  $dE/dx$  sampling in the IMC** allow to **identify individual nuclear species** ( $\Delta z \sim 0.15-0.3 e$ ).
- ❑ **IMC**: a **high granularity (1mm) imaging pre-shower calorimeter** accurately identifies the **arrival direction** of incident particles ( $\sim 0.1^\circ$ ) and the **starting point** of electro-magnetic showers.
- ❑ **TASC**: a thick ( $\sim 30 X_0$ ), **fully active calorimeter** allows to extend electron measurements into the TeV energy region with  $\sim 2\%$  **energy resolution**.
- ❑ **Combined**, they **separate electrons** from the abundant protons (rejection  $> 10^5$ ).

Simulated Shower Profile

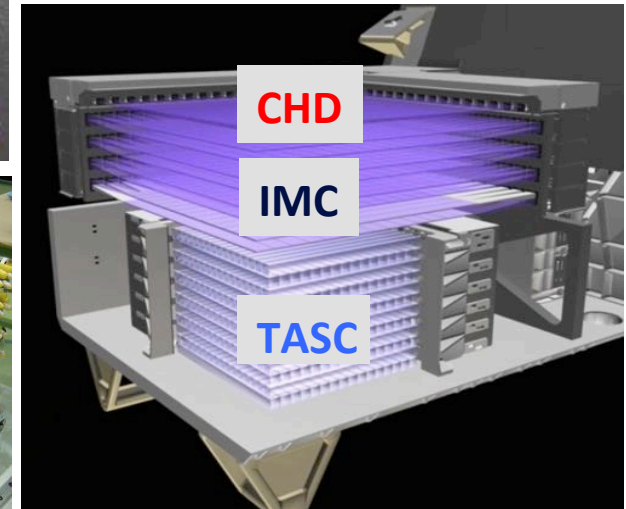
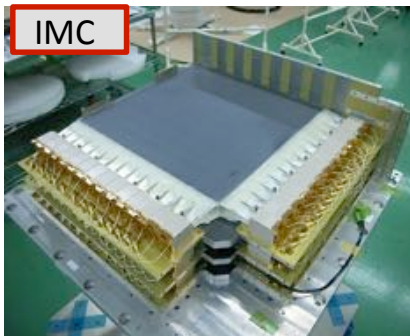
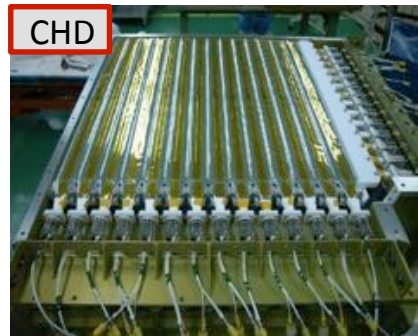




# CALET Instrument



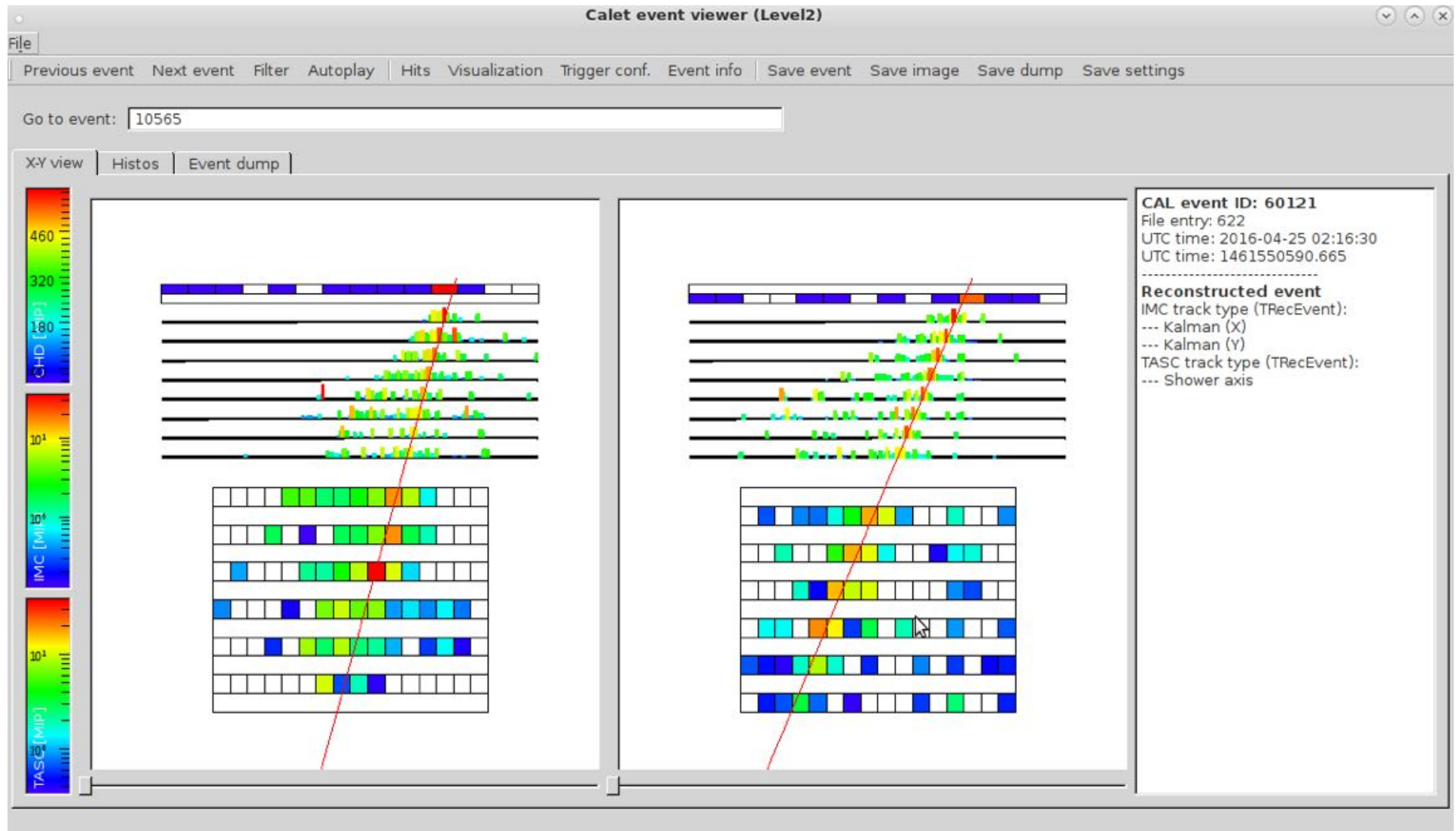
## CALORIMETER



	CHD (Charge Detector)	IMC (Imaging Calorimeter)	TASC (Total Absorption Calorimeter)
Measure	Charge (Z=1-40)	Tracking , Particle ID	Energy, e/p Separation
Geometry (Material)	Plastic Scintillators: 28 paddles 14 paddles x 2 layers (X,Y) Paddle Size: 32 x 10 x 450 mm <sup>3</sup>	Scintillating Fibers: 448 x 16 layers (X,Y) 7 W layers (3X <sub>0</sub> ): 0.2X <sub>0</sub> x 5 + 1X <sub>0</sub> x 2 Scifi size: 1 x 1 x 448 mm <sup>3</sup>	PWO logs: 16 x 12 layers (x,y): 192 logs log size: 19 x 20 x 326 mm <sup>3</sup> Total Thickness: 27 X <sub>0</sub> , ~1.2 λ <sub>i</sub>
Readout	PMT+CSA	64-anode PMT+ ASIC	APD/PD+CSA PMT+CSA (for Trigger)@top layer

✧ CALET **tracking** takes advantage of the IMAGING capabilities of IMC thanks to its granularity of 1 mm with Sci-fibers **readout individually**.

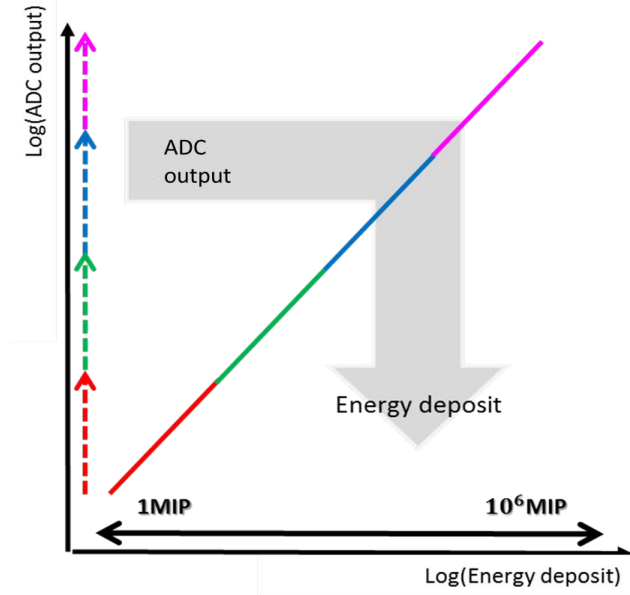
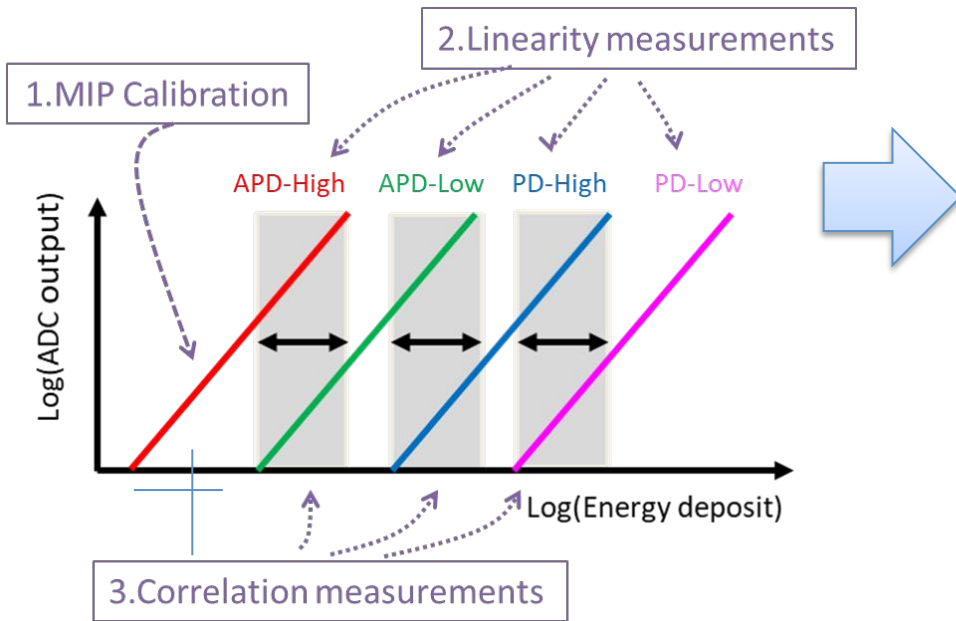
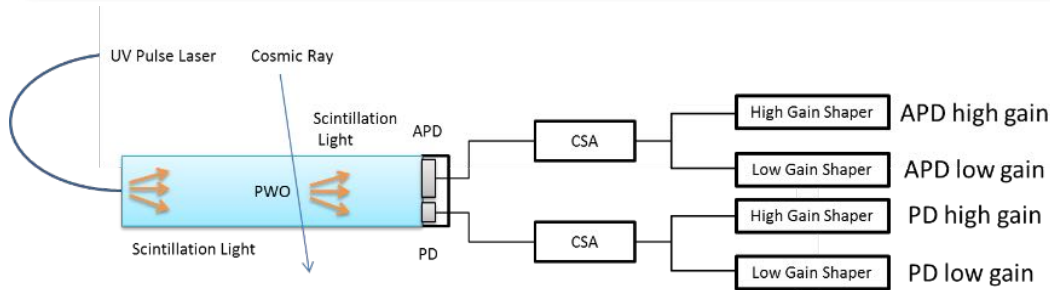
**Example:** A multi-prong event due to an interaction of the primary particle in the CHD is very well imaged by the IMC.



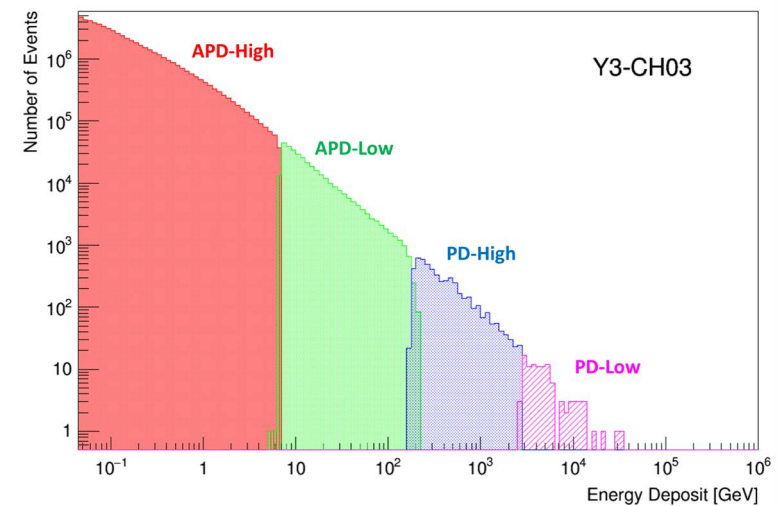




# TASC Energy Measurement: wide Dynamical Range 1-10<sup>6</sup> MIPs



Example of energy measurement in one log of TASC

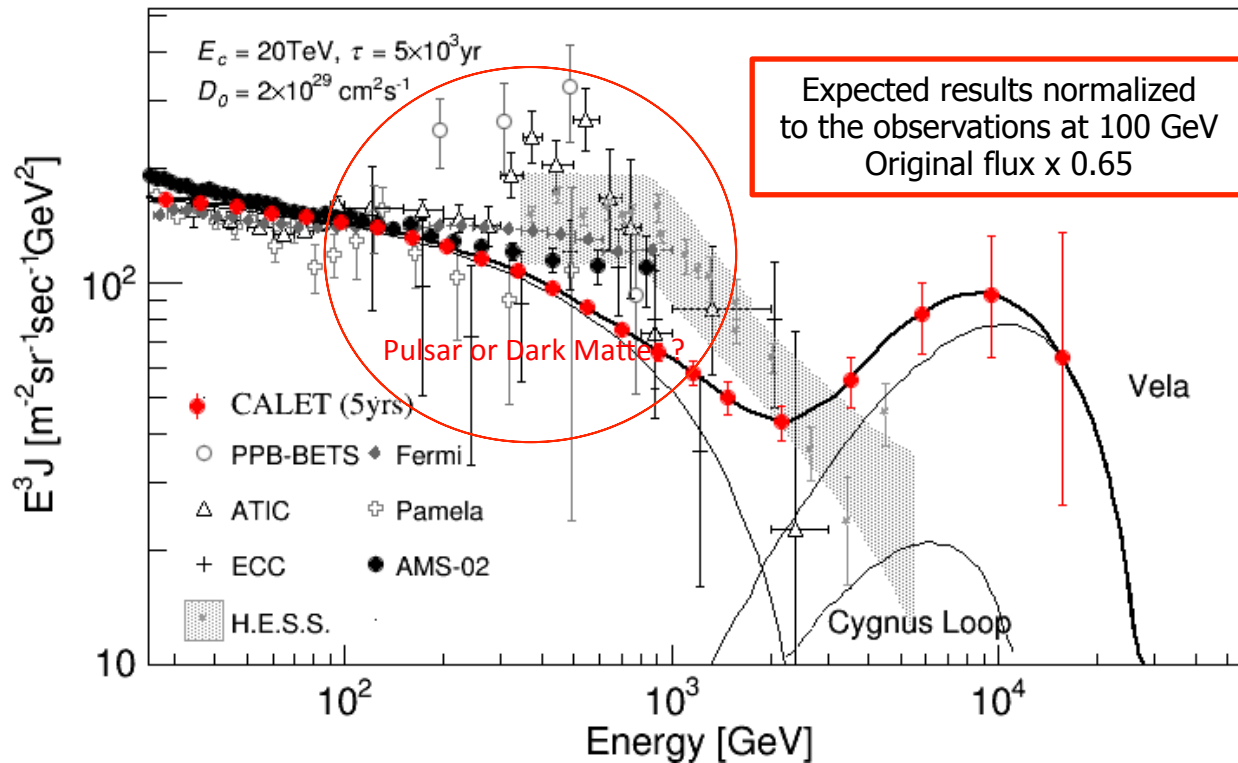


Details of our energy calibration can be found at:  
 Y.Asaoka, Y.Akaike, Y.Komiya, R.Miyata, S.Torii et al.,  
 Astropart. Phys. 91 (2017) 1.

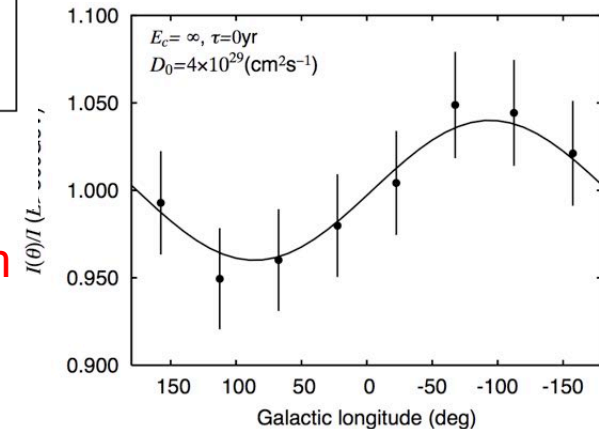
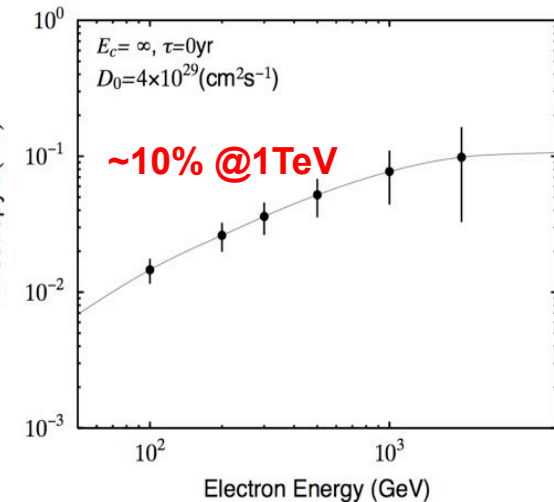


# CALET Main Target: Identification of Electron Sources

Some nearby sources, e.g. Vela SNR, are likely to have unique signatures in the electron energy spectrum at the TeV scale (Kobayashi et al. ApJ 2004)

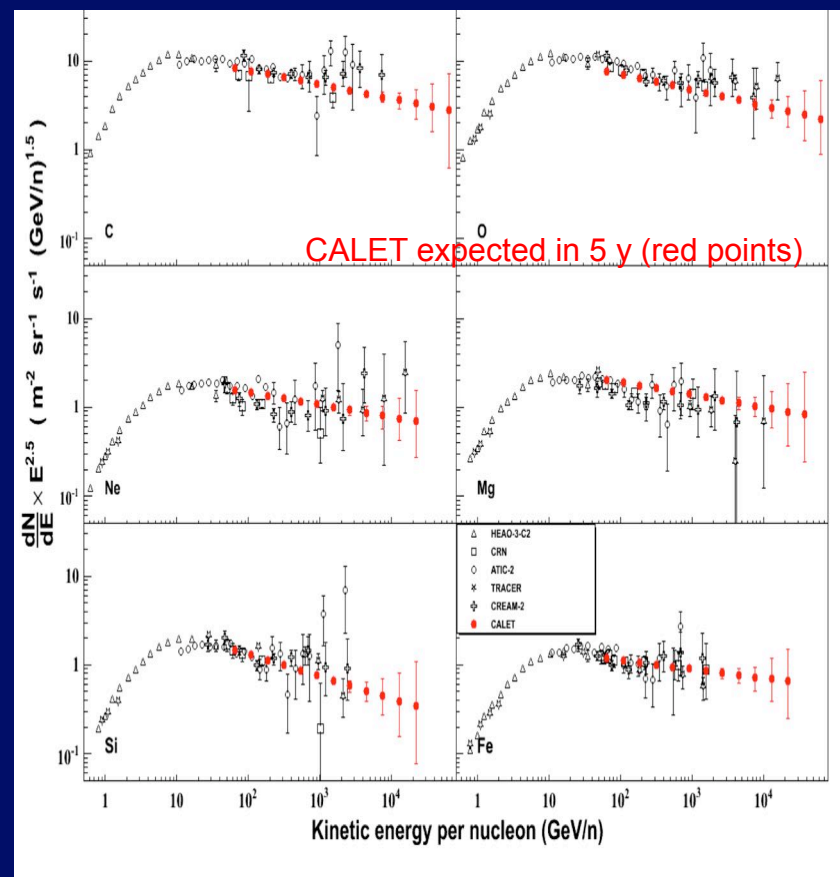
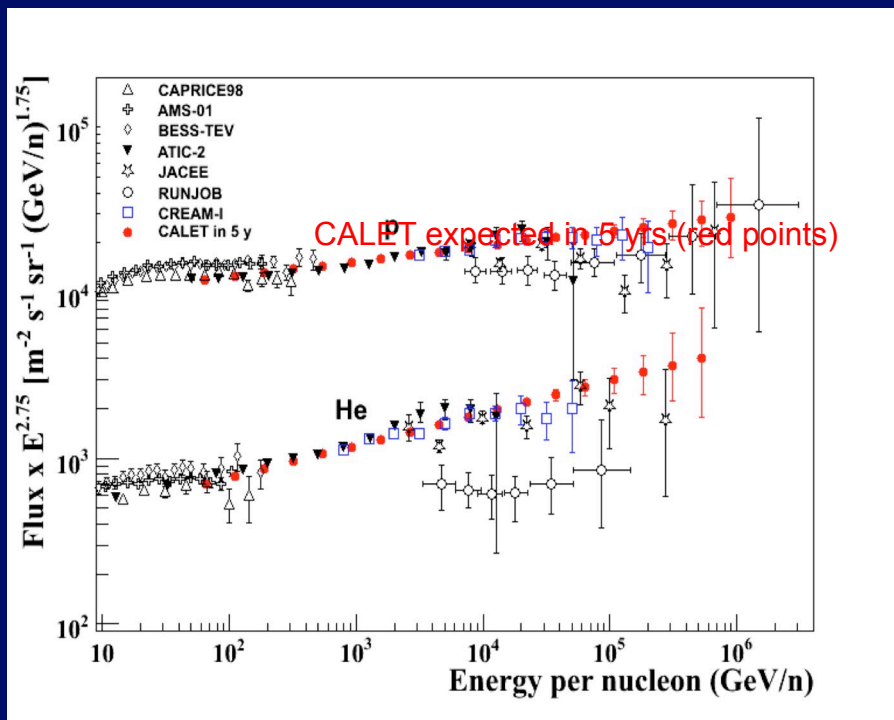


Expected Anisotropy from Vela



possible identification of the unique signature from nearby SRNs, such as Vela, in the electron spectrum by CALET in the TeV region

# CALET: Cosmic-Ray Nuclei Spectra in the Multi-TeV region



- Proton spectrum to  $\approx 900$  TeV
- He spectrum to  $\approx 400$  TeV/n
- Spectra of C,O,Ne,Mg,Si to  $\approx 20$  TeV/n
- B/C ratio to  $\approx 4 - 6$  TeV/n
- Fe spectrum to  $\approx 10$  TeV/n

CALET energy reach  
(5 years)



# Main Scientific Objectives

Scientific Objectives	Observation Targets	Energy Range
CR Origin and Acceleration	Electron spectrum p→Fe individual spectra Ultra Heavy Ions ( $26 < Z \leq 40$ ) Gamma-rays (Diffuse + Point sources)	1 GeV - 20 TeV 10 GeV - 1000 TeV > 600 MeV/n 1 GeV - 1 TeV
Galactic CR Propagation	B/C and sub-Fe/Fe ratios	Up to some TeV/n
Nearby CR Sources	Electron spectrum	100 GeV - 20 TeV
Dark Matter	Signatures in electron/gamma-ray spectra	100 GeV - 20 TeV
Solar Physics	Electron flux (1 GeV-10 GeV)	< 10 GeV
Gamma-ray Transients	Gamma-rays and X-rays	7 keV - 20 MeV

- ❑ Electron observation in 1 GeV - 20 TeV is achieved with high energy resolution due to design optimization for electron detection **Search for Dark Matter and Nearby Sources**
- ❑ Observation of cosmic-ray nuclei will be performed in energy region from 10 GeV to 1 PeV **Unravelling the CR acceleration and propagation mechanism(s)**
- ❑ Detection of transient phenomena in space by stable observations **Gamma-ray bursts, Solar flares, e.m. counterpart from GW sources, ...**

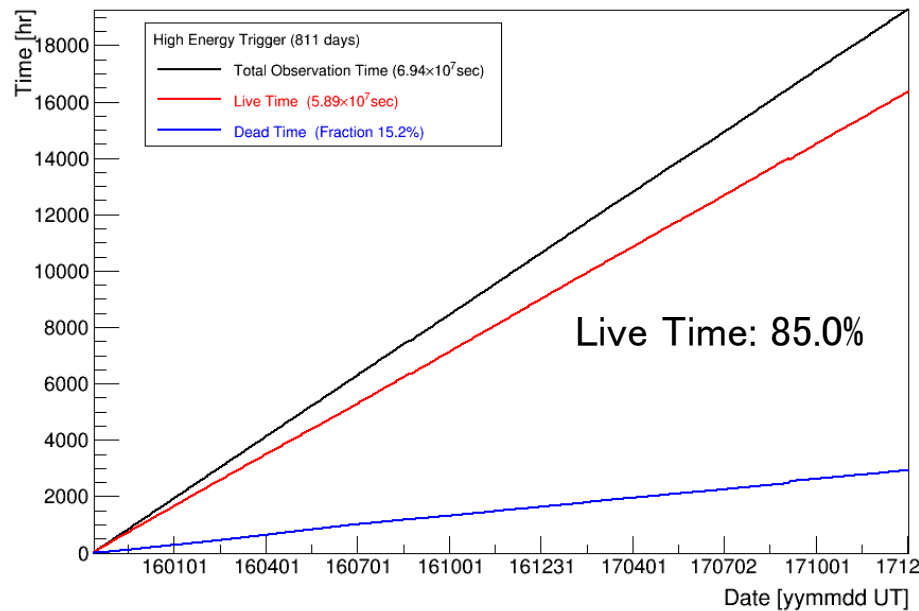


# Observation by High Energy Trigger (>10GeV)

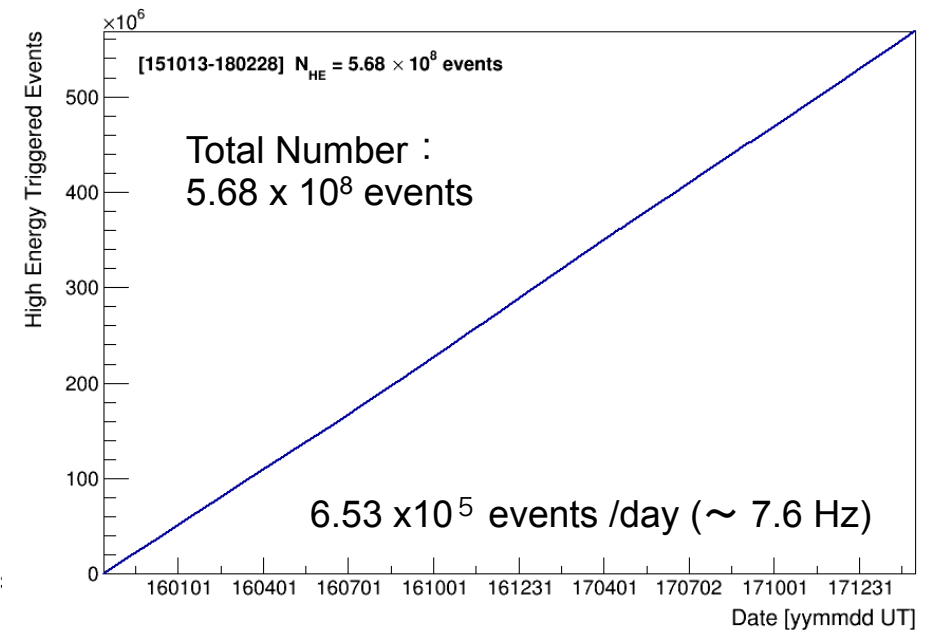
Observation by High Energy Trigger for 870 days : Oct.13, 2015 – Dec.31, 2017

- The exposure,  $S\Omega T$ , has reached to  $\sim 76.0 \text{ m}^2 \text{ sr day}$  for electron observations by continuous and stable operations.
- Total number of the triggered events is  $\sim 570 \text{ million}$  with a live time fraction of 85.0 %.

Accumulated observation time (live, dead)



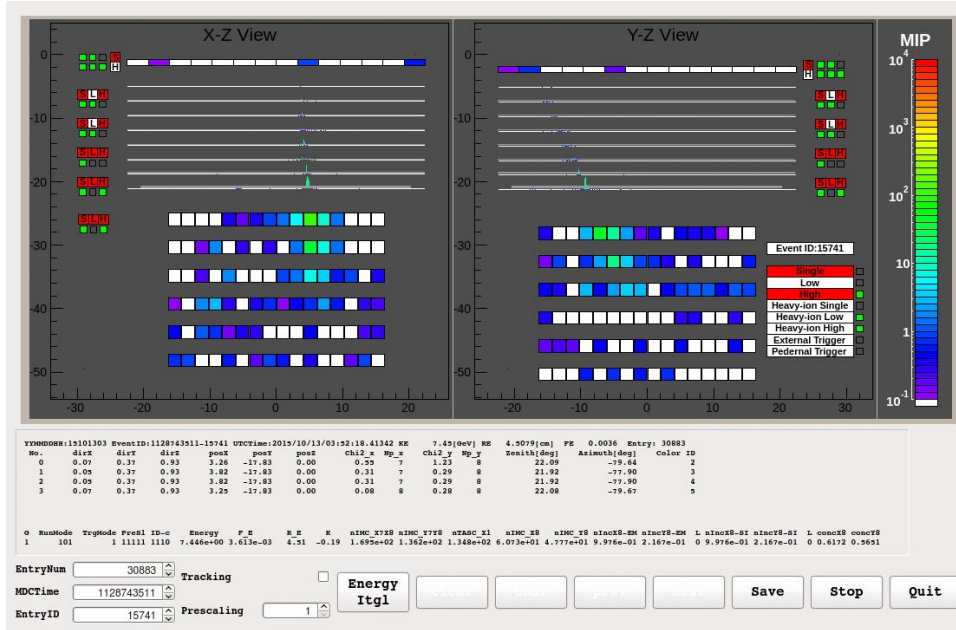
Accumulated triggered event number



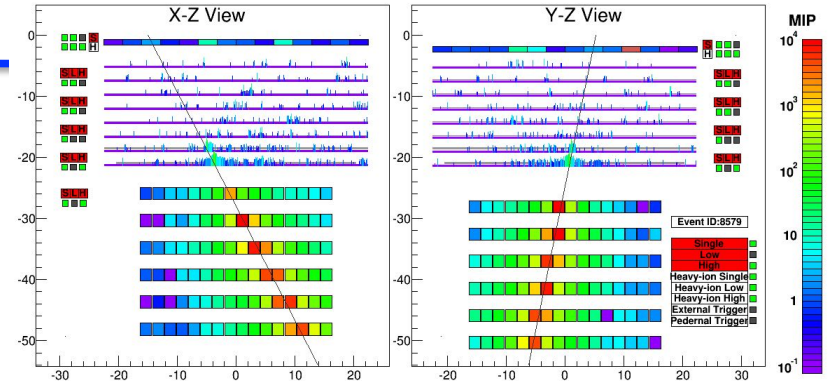


# Examples of Observed Events

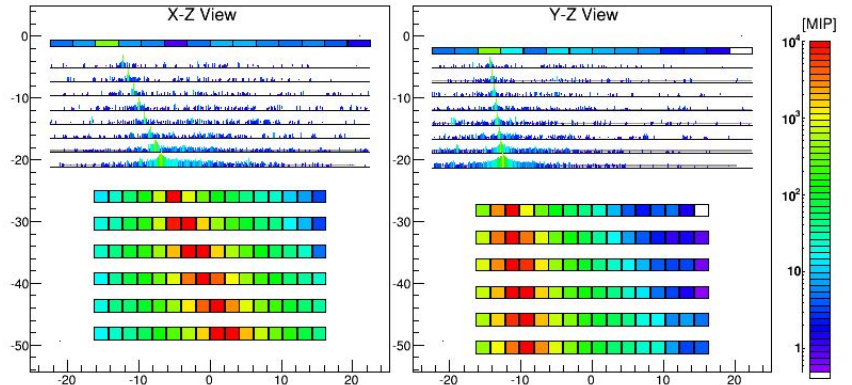
## Event Display: Electron Candidate (>100 GeV)



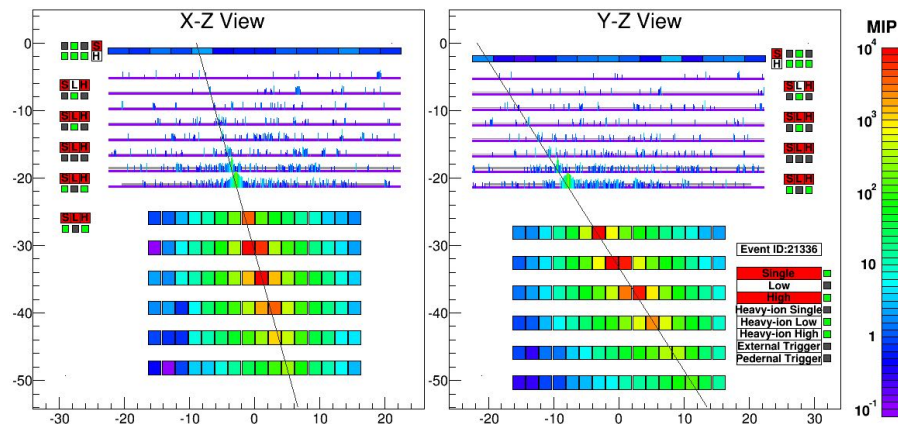
## Proton, $\Delta E=2.89$ TeV



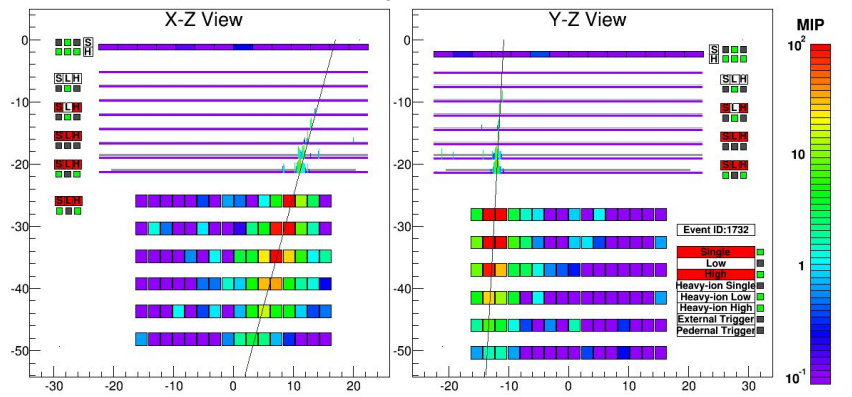
## Fe, $\Delta E=9.3$ TeV



## Electron, $E=3.05$ TeV



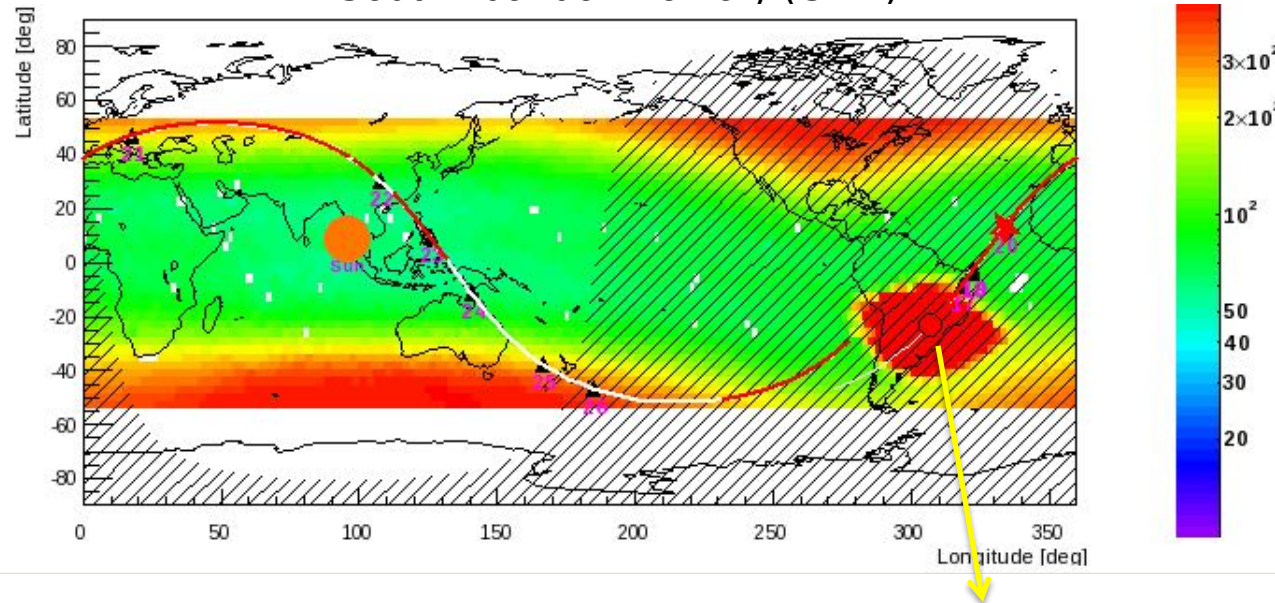
## Gamma-ray, $E=44.3$ GeV





# ISS Radiation Environment

### South Atlantic Anomaly (SAA)

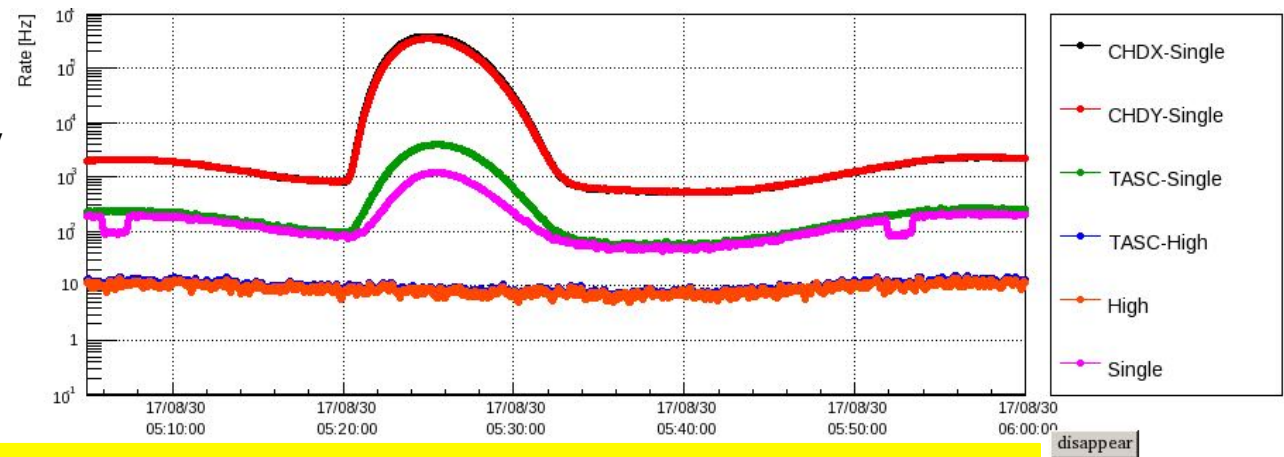


ISS orbit  
@ 2017/08/29 5:25UT  
 ISS ran through SAA.

CHD count rate jumped up to  $\sim 3 \times 10^5$  Hz from  $10^3$  Hz, but the HE trigger rate remained stable.

### Trigger/Count Rate @ 2017/08/29

HE trigger was not affected by SAA thanks to high energy threshold ( $>10$  GeV).  
 (Energies of the trapped particles are too low to make a trigger for the observations.)

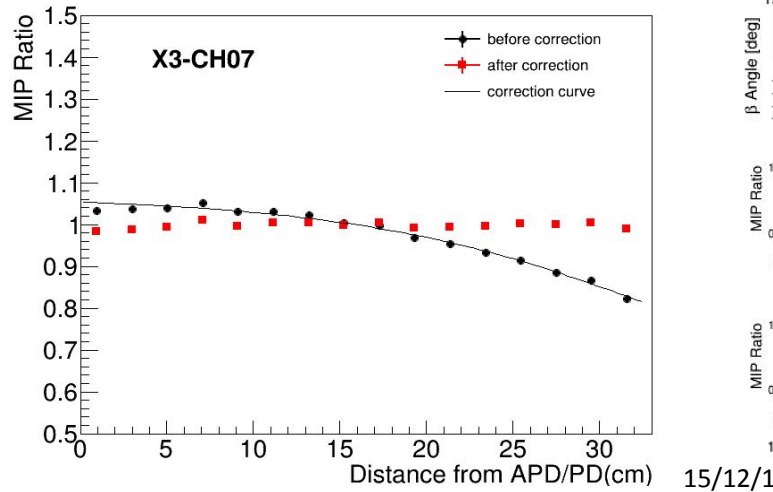


**⇒ Observation is continuously carried out even at SAA!**

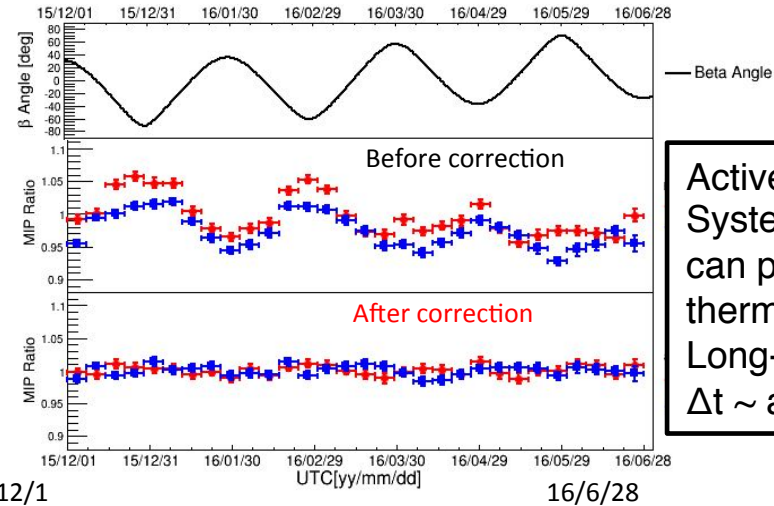


# Position and Temperature Calibration, and Long-term Stability

Example of **position dependence** correction



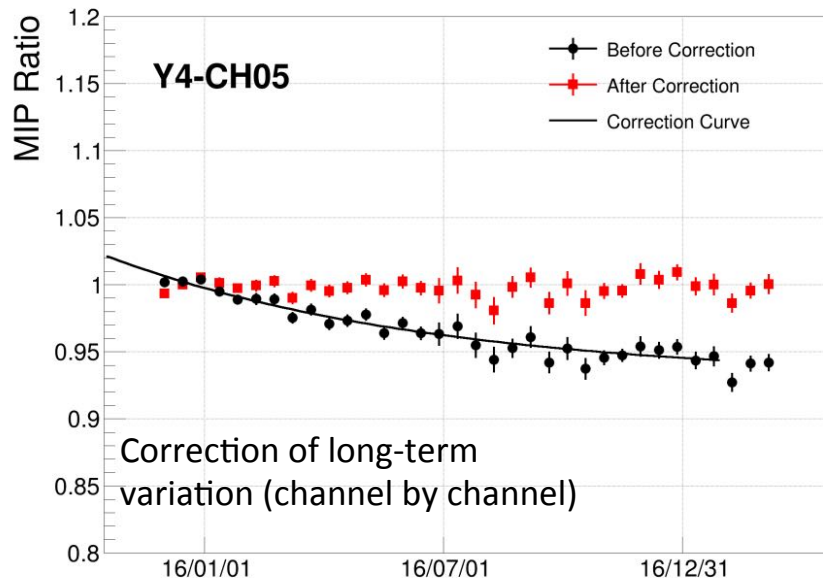
Examples of **temperature change** correction



**TASC**

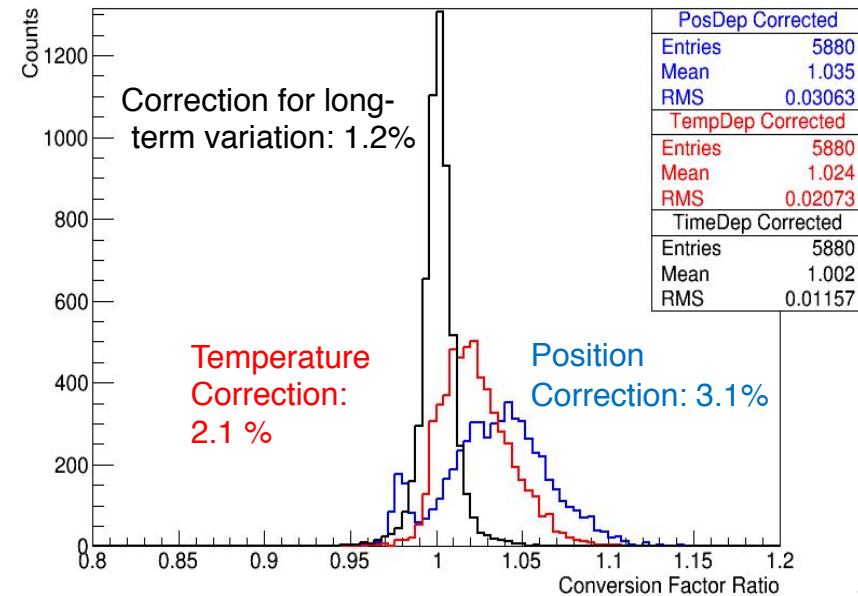
Active Thermal Control System (ATCS) on ISS can provide very stable thermal condition during Long-term observations:  $\Delta t \sim$  a few degrees

Example of **long-term variation** correction



Correction of long-term variation (channel by channel)

Distribution of MIPs for 192 ch x 16 segmented positions after each correction





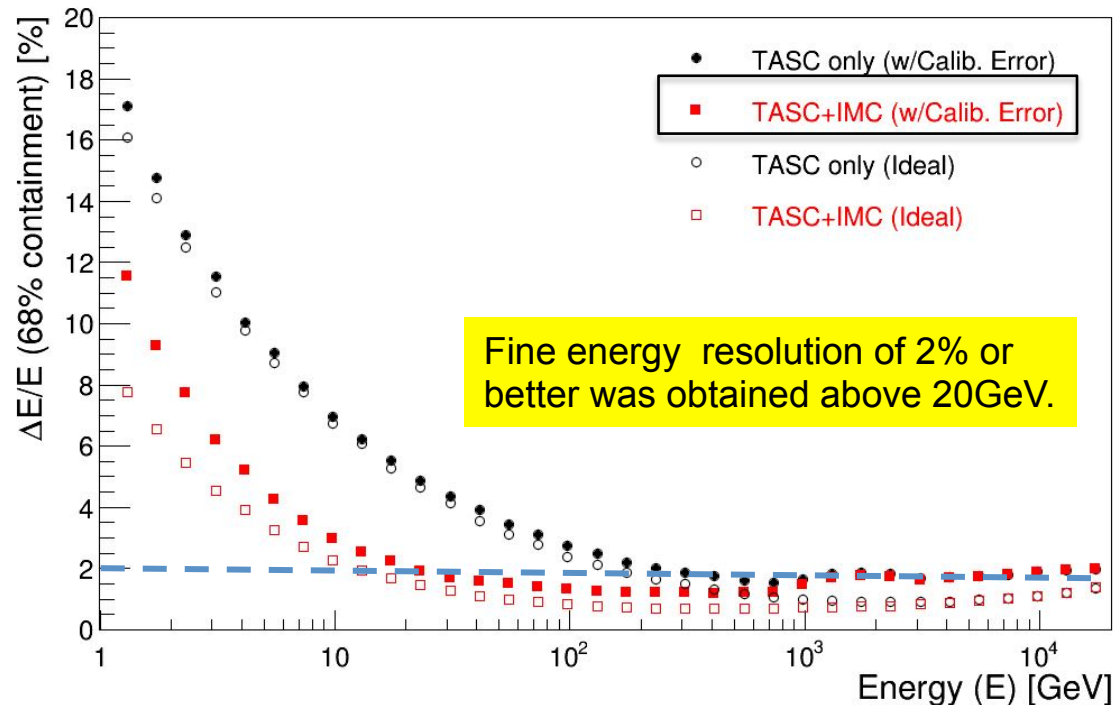


# Energy Resolution for Electrons by On-orbit Calibration

**Y.Asaoka, Y.Akaike, Y.Komiya, R.Miyata, S.Torii et al.,  
Astroparticle Physics 91 (2017) 1.**

Considering the calibration errors and instrument noise, energy resolution is estimated as a function of energy.

## Energy dependence of energy resolution

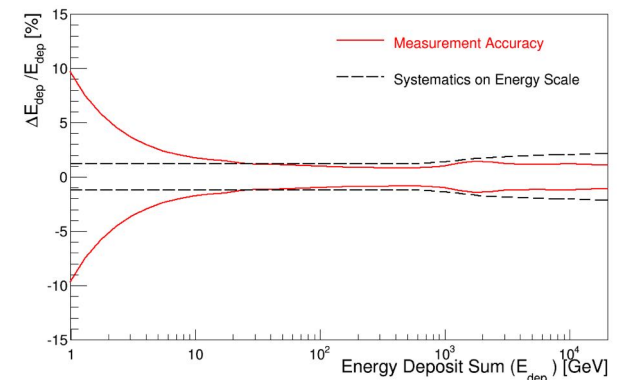


## Error budget in energy calibration

MIP	Energy conversion	2.6%
	Peak fitting of MC and flight data	0.6%
	Fitting range dependence	0.6% <sup>(*)</sup>
	Position dependence	1.8%
	Temperature dependence	1.0%
	Rigidity cutoff dependence	1.0% <sup>(*)</sup>
	Systematic uncertainty estimated from p/He consistency	1.0%
UV Laser	Linearity	1.4~2.5%
	Fit error	
	APD high gain	1.4%
	APD low gain	1.5%
	PD high gain	2.5%
	PD low gain	2.2%
Gain Ratio	Gain range connection	1.6~2.1%
	Fit error	
	APD-high to APD-low gain	0.1%
	APD-low to PD-high gain	0.7%
	PD high to PD low gain	0.1%
	Slope extrapolation	
	APD-high to APD-low gain	1.6%
	APD-low to PD-high gain	2.0% <sup>(*)</sup>
	PD high to PD low gain	1.8%
Sampling Bias		0.5% <sup>(**)</sup>

<sup>(\*)</sup> also considered as systematic error on energy scale

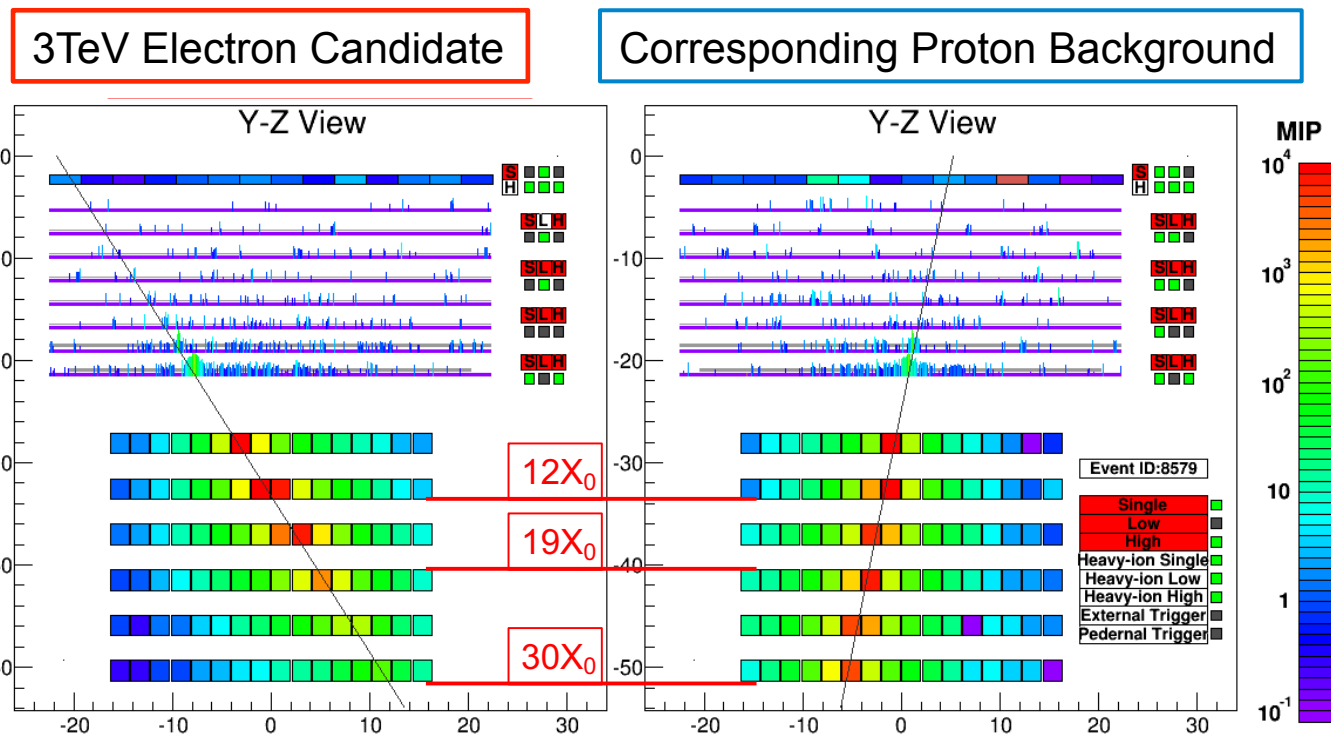
<sup>(\*\*)</sup> energy-scale systematic error only





# Electron Analysis: Characteristics of TeV Electron and Proton Showers

Simple and high-efficiency electron identification is possible even at TeV.  
⇒ CALET is best suited for observation of **possible narrow structures** in the total electron spectrum in the trans-TeV region.





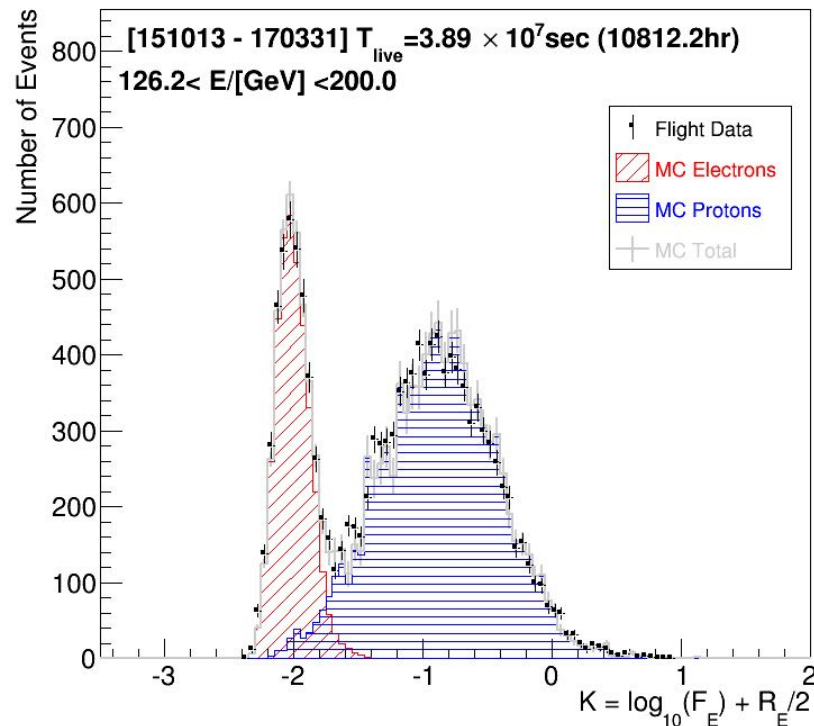
# Electron / Proton Separation

## Simple Two Parameter Cut

- $F_E$ : Energy fraction of the bottom layer sum to the whole energy deposit sum in TASC
- $R_E$ : Lateral spread of energy deposit in TASC-X1

Cut Parameter K is defined as follows:

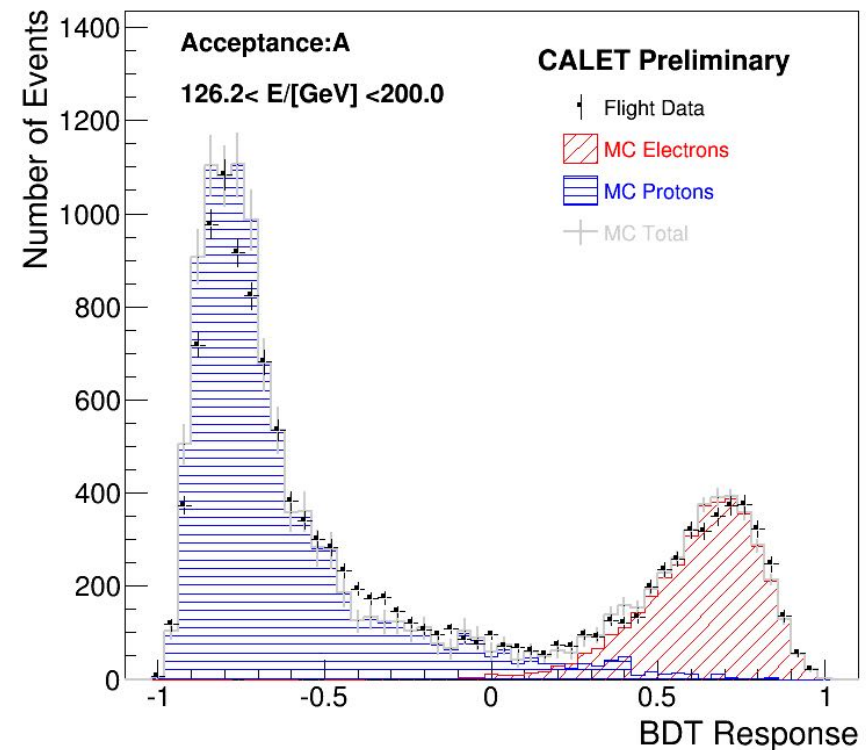
$$K = \log_{10}(F_E) + 0.5 R_E (\text{/cm})$$



## Boosted Decision Trees (BDT)

In addition to the two parameters in the left, TASC and IMC shower profile fits are used as discriminating variables

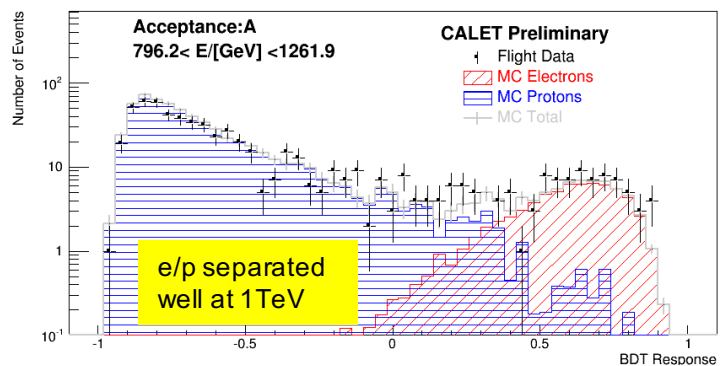
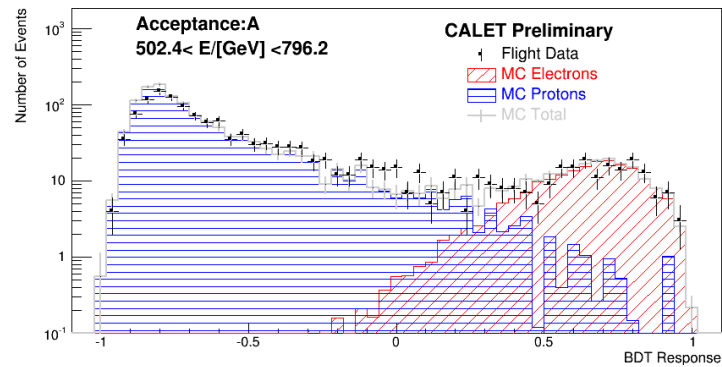
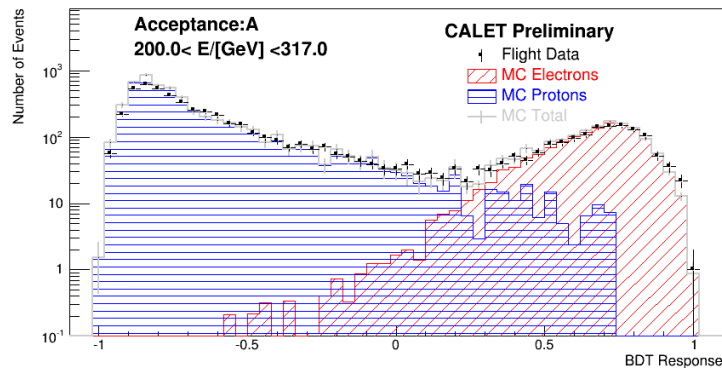
**BDT Response using 9 parameters**



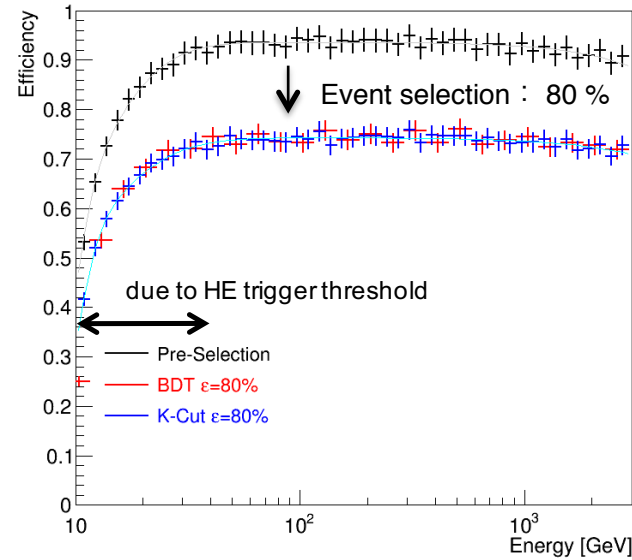


# e/p Discrimination Power by Analysis of BDT and K parameter

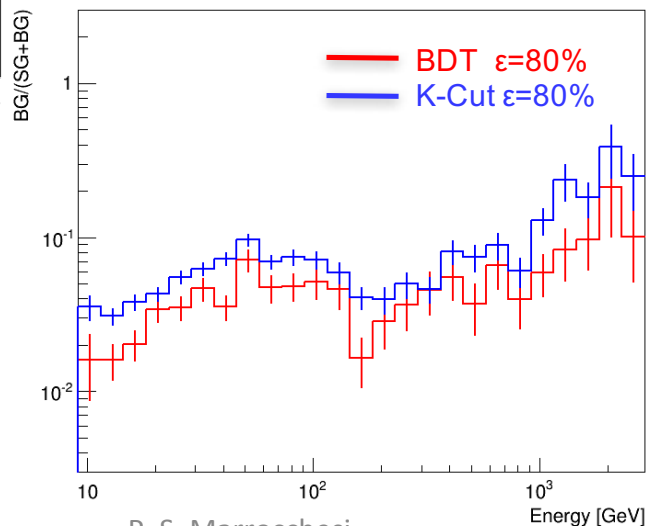
## Distribution of BDT Response



## Electron Efficiency



## Proton contamination Ratio



- KEY POINT: high and almost energy independent efficiency
- The efficiencies of K-cut and BDT have very similar energy dependence.
- Electron efficiency after pre-selection and e/p separation is considerably high (~70%) and ~constant above HE trigger threshold.
- Simple two parameter cut is used in the lower energy region (< 500GeV), while the difference in resultant spectrum are taken into account in the systematic uncertainty.
- proton contamination is 2 - 5 % in 10 GeV-1 TeV, 5-10 % above 1 TeV with BDT analysis. (improving with analysis)

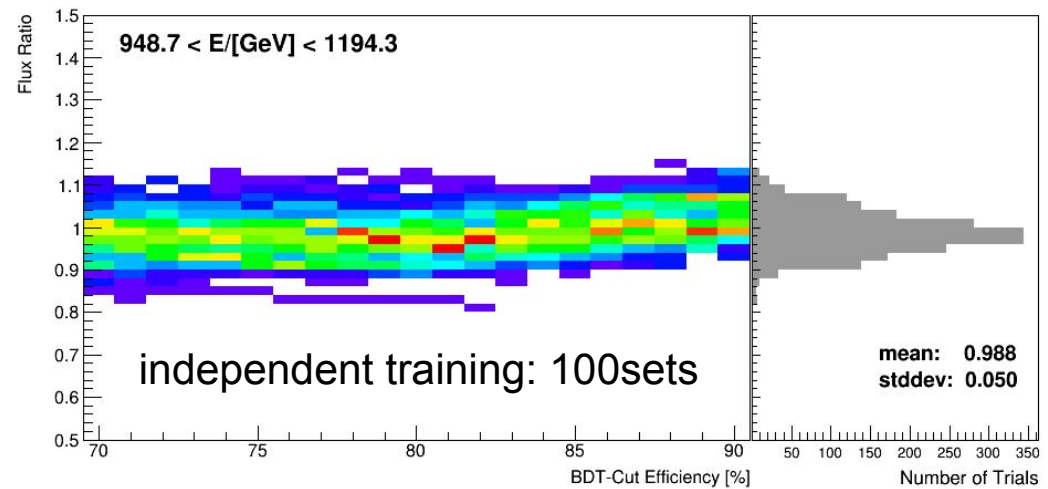


# Systematic Uncertainties in Derivation of Energy Spectrum

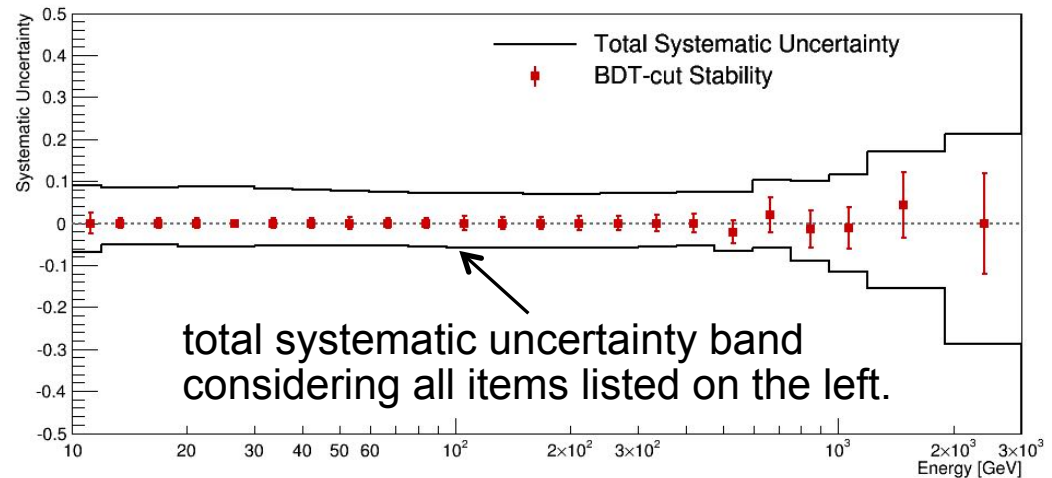
Stability of resultant flux are intensively studied in the large parameter space (i.e., viable choices to derive spectrum)

- Normalization:
  - Live time
  - Radiation environment
  - Long-term stability
  - Quality cuts
- Energy dependent:
  - Tracking
  - charge ID
  - electron ID (K-Cut vs BDT)
  - BDT stability (vs efficiency & training)
  - MC model (EPICS vs Geant4)

Systematic uncertainty in electron selection by BDT



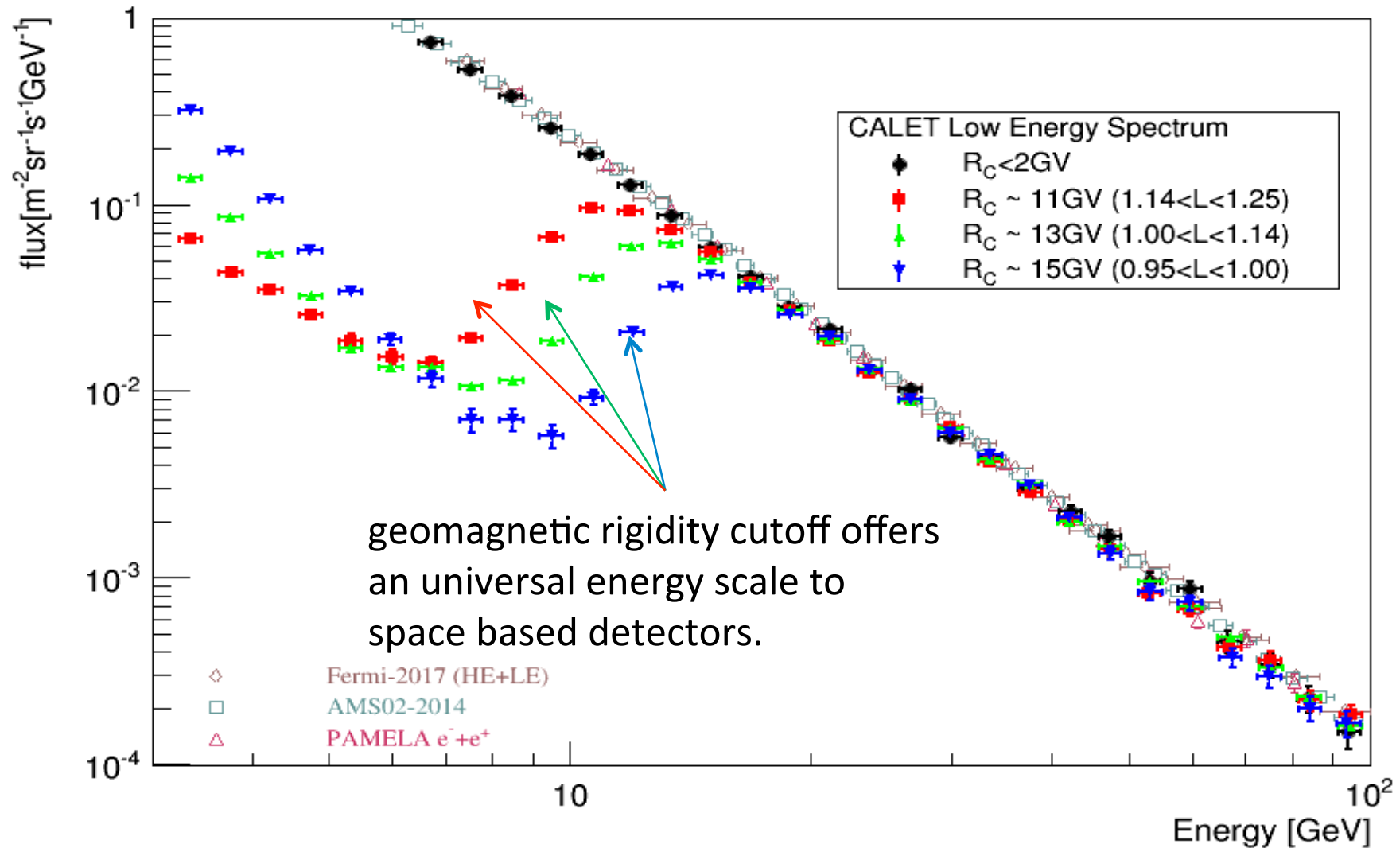
Total systematic uncertainty vs Energy



N.B. Energy scale uncertainty is not included in this analysis.



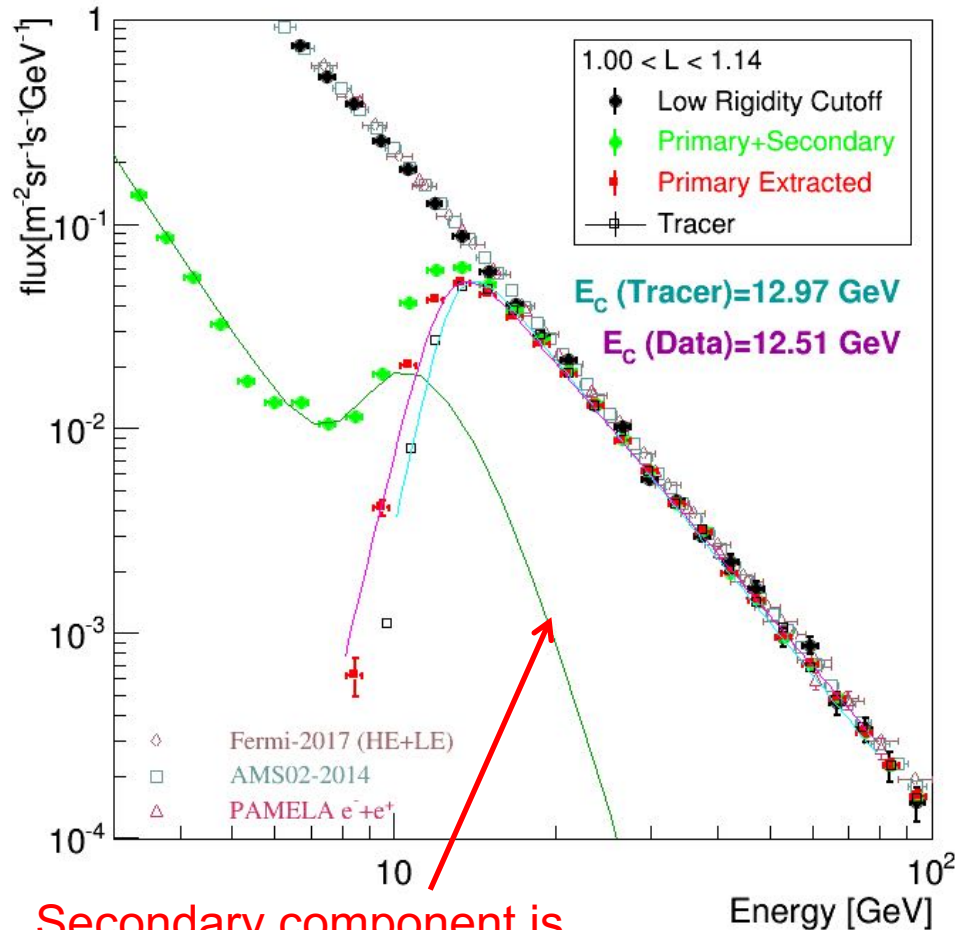
# Calibration of Absolute Energy Scale Using Geomagnetic Rigidity Cutoff Energy





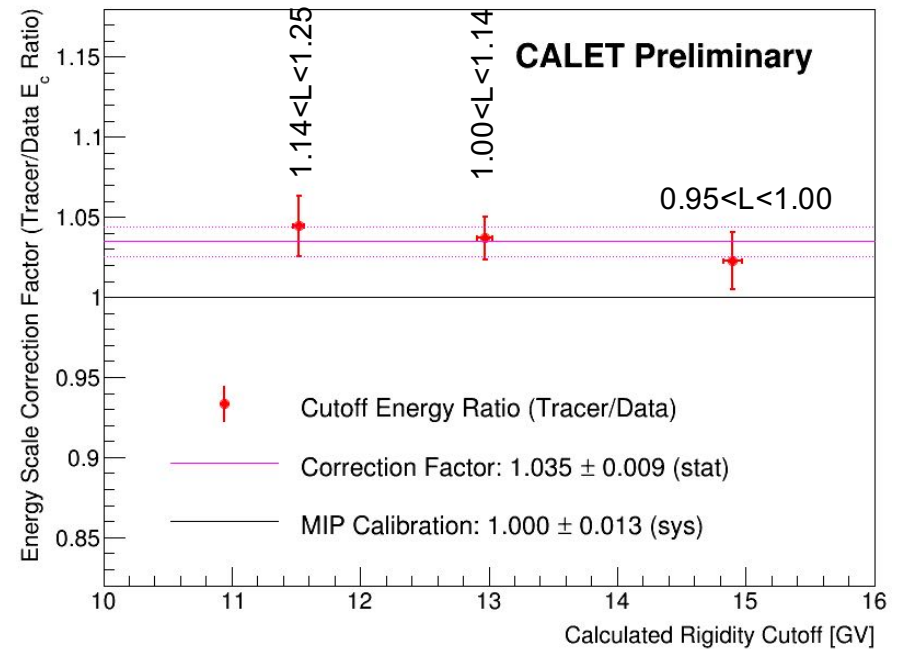
# Cutoff Rigidity Measurements and Comparison with Calculation

## BEFORE CORRECTION



Secondary component is estimated using azimuthal distributions

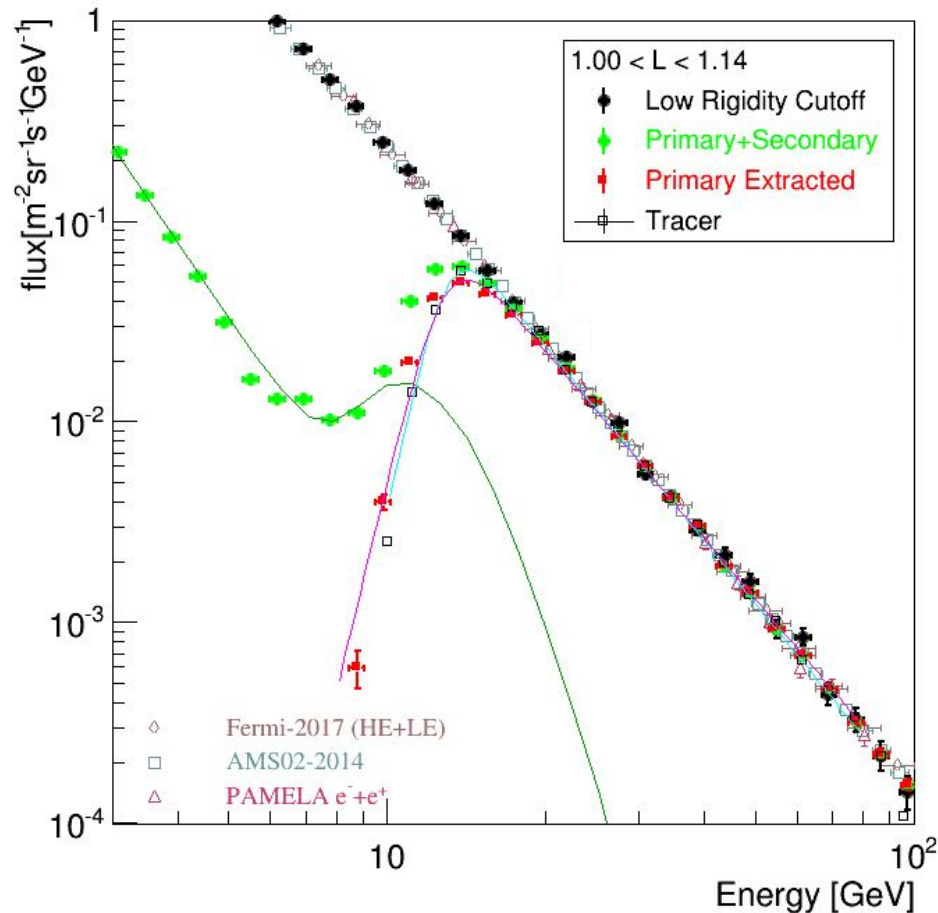
- Performed in three different cutoff rigidity regions.
- Correction factor was found to be **1.035** compared to MIP calibration.



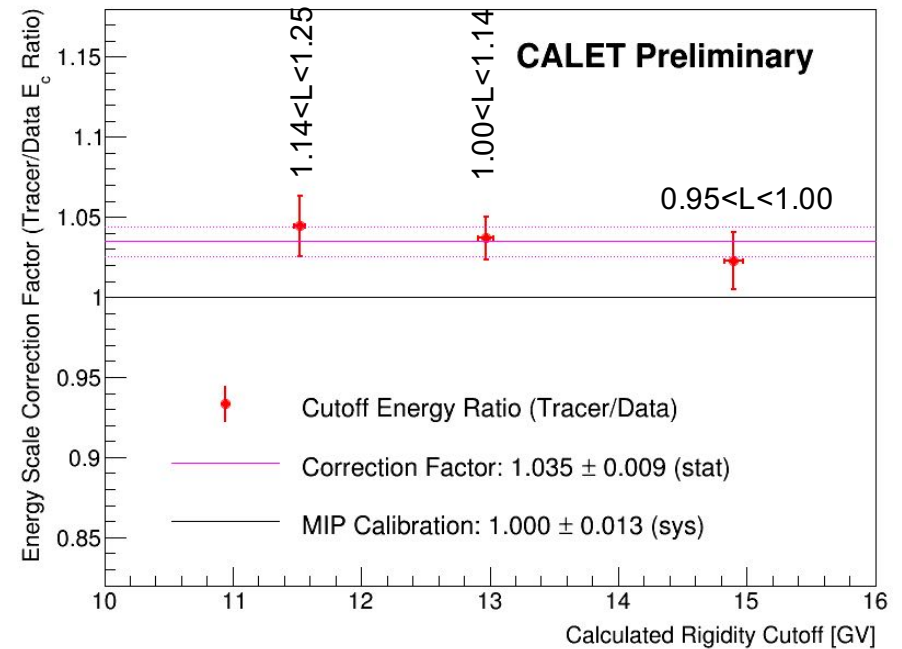


# Cutoff Rigidity Measurements and Comparison with Calculation

## AFTER CORRECTION



- Performed in three different cutoff rigidity regions.
- Correction factor was found to be **1.035** compared to MIP calibration.



Since universal energy-scale calibration between different instruments is very important, we adopt the energy scale determined by rigidity cutoff to derive our spectrum.

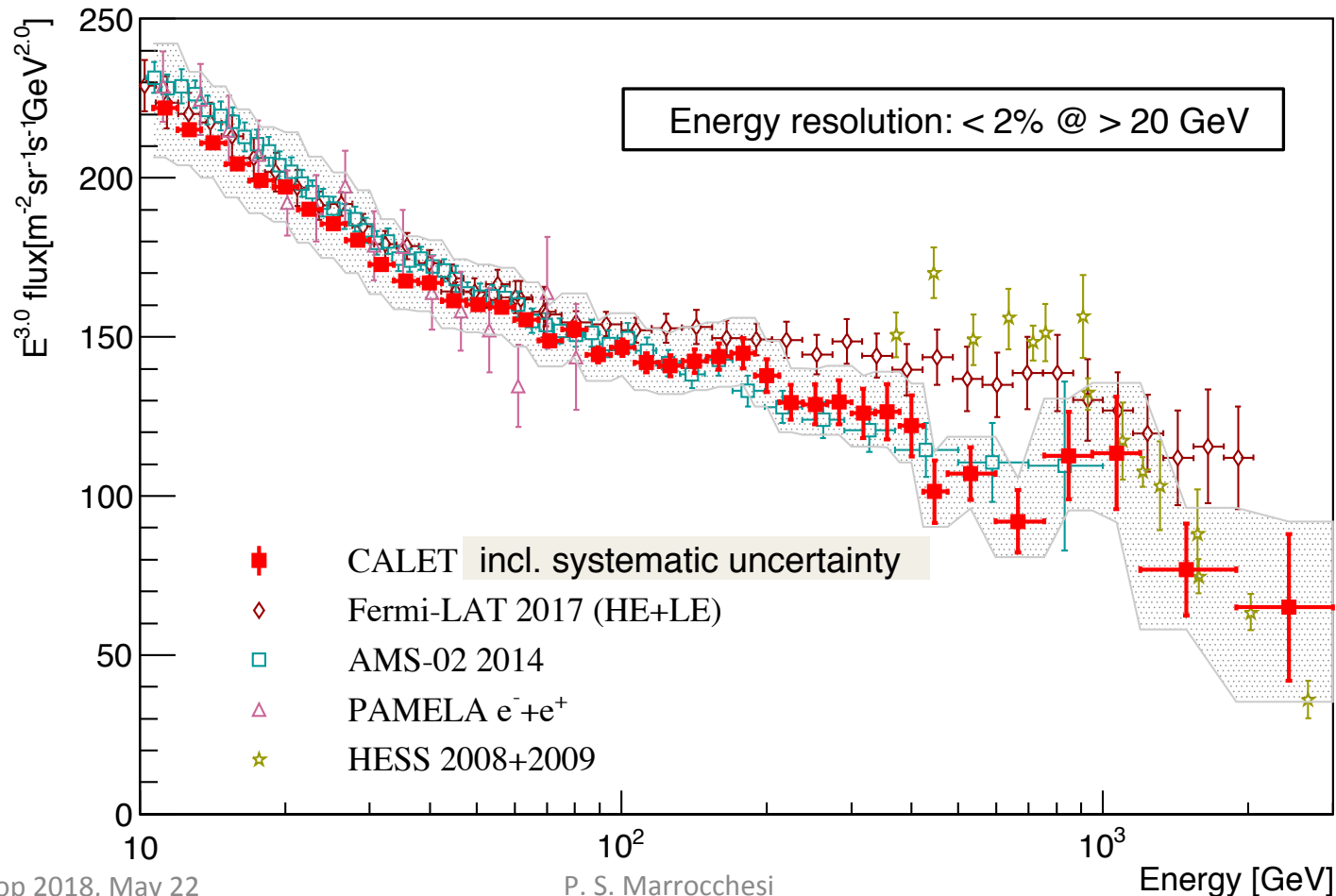




# Total ( $e^+e^-$ ) Electron Energy Spectrum in 10 GeV $\sim$ 3TeV

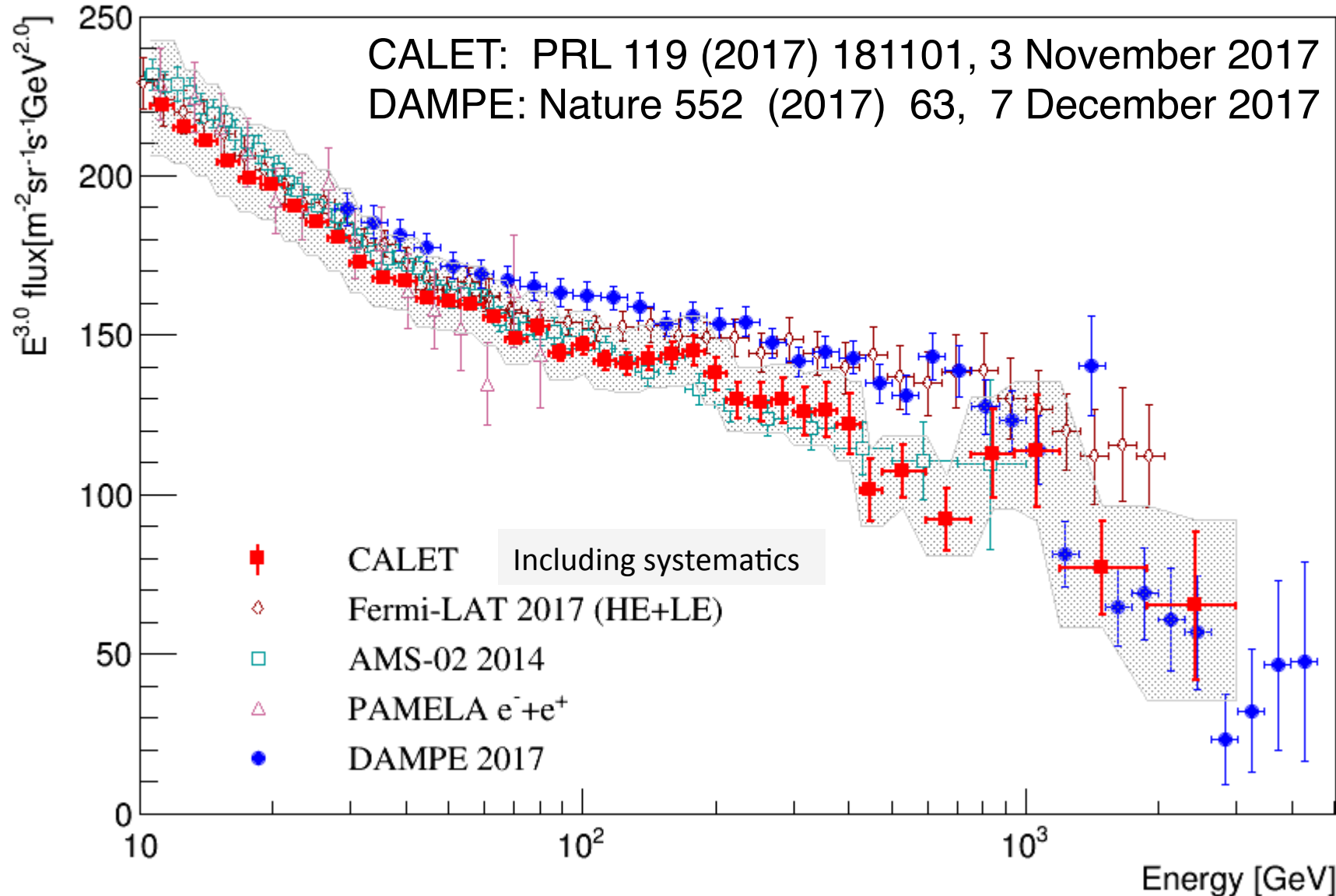
- Geometry Condition:  $S\Omega = 570.3 \text{ cm}^2\text{sr}$  (Fully Contained: 55% for all acceptance)
- Live Time: 2015/10/13—2017/06/30 (x 0.85)  $\Rightarrow T = 4.57 \times 10^7 \text{ sec}$
- Exposure:  $S\Omega T = 2.64 \times 10^6 \text{ m}^2 \text{ sr sec}$  (**less than 20% of full analysis for 5 years**)

Physical Review Letters 119 (2017) 181101, 3 November 2017



# All-Electron Spectrum Comparison w/ DAMPE

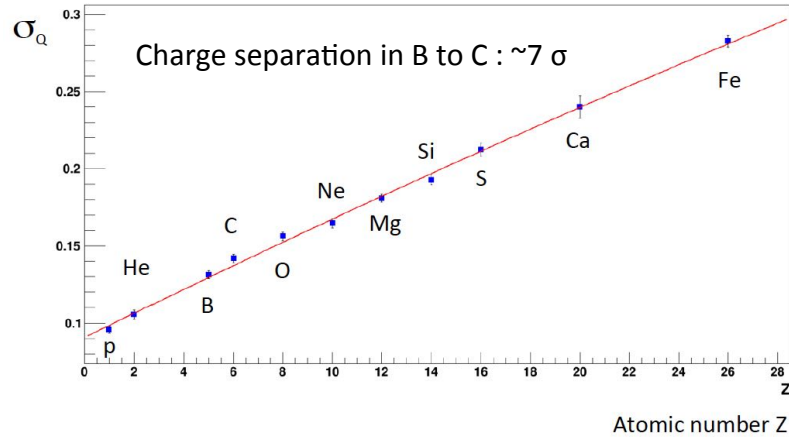
We are trying to increase our statistics by a factor of  $\sim 2$  using full acceptance.



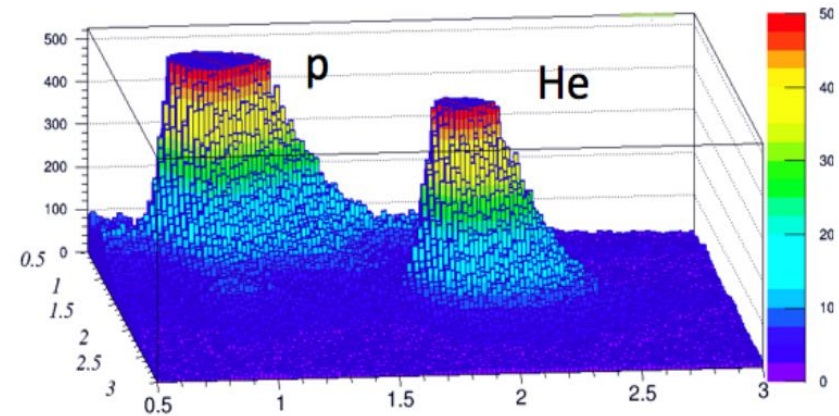


# Preliminary Nuclei Measurements for Z=1-8

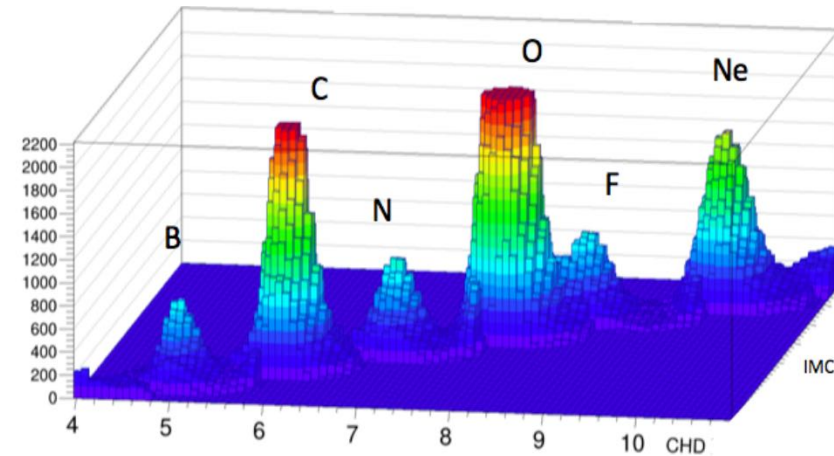
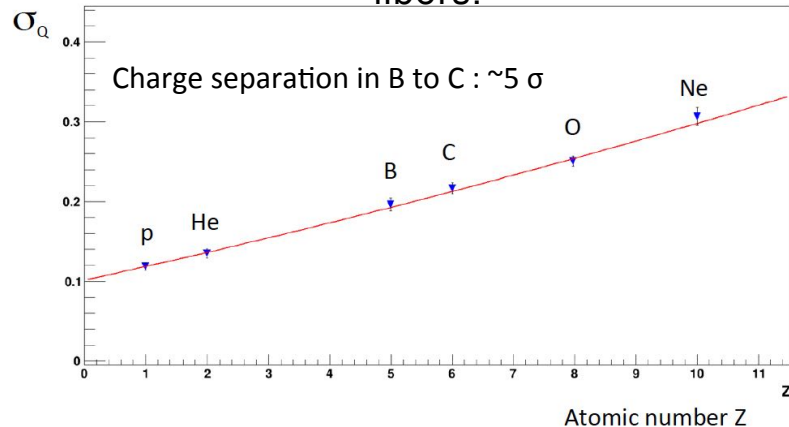
CHD charge resolution (2 layers combined) vs. Z



Charge resolution combined CHD+IMC



Charge resolution using multiple dE/dx measurements from the IMC scintillating fibers.



Non-linear response to  $Z^2$  is corrected both in CHD and IMC using a model.

\*) Plots are truncated to clearly present the separation.

A clear separation between p, He,  $\sim Z=8$ , can be seen from CHD+IMC data analysis.



# Preliminary Heavy Nuclei Energy Spectrum

Flux measurement:  $\Phi(E) = \frac{N(E)}{S\Omega\varepsilon(E)T\Delta E}$

$N(E)$ : Events in unfolded energy bin

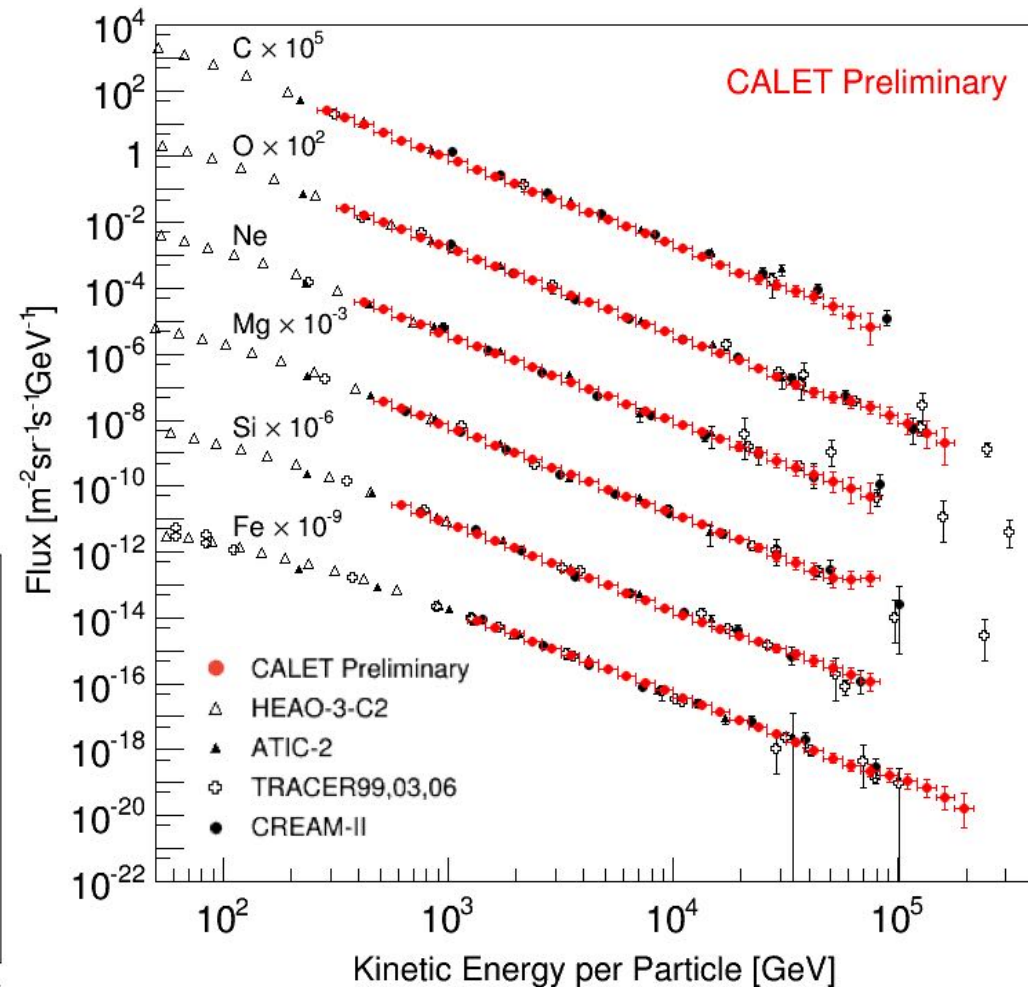
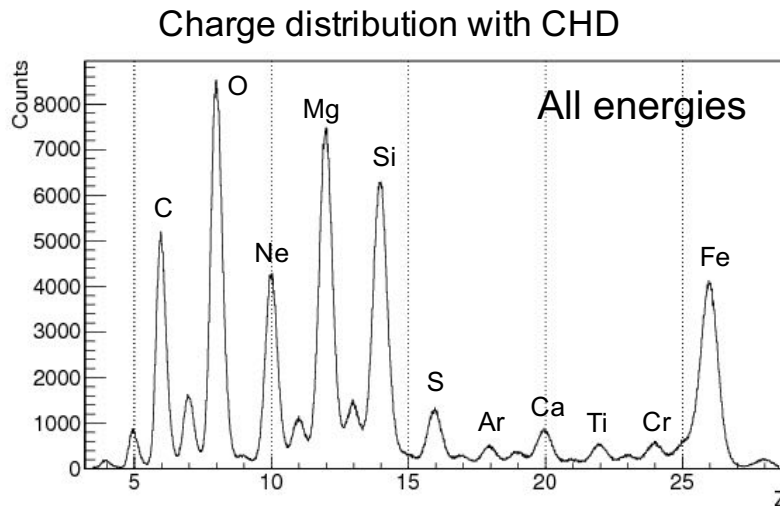
$S\Omega$  : Geometrical acceptance  
(A+B: 570 cm<sup>2</sup>sr)

$T$  : Live time (39 million seconds)  
(Oct.13, 2015 – Mar. 31, 2017)

$\varepsilon(E)$  : Efficiency of trigger and track reconstruction (>96%)

$\Delta E$  : Energy bin width

Energy spectrum per particle

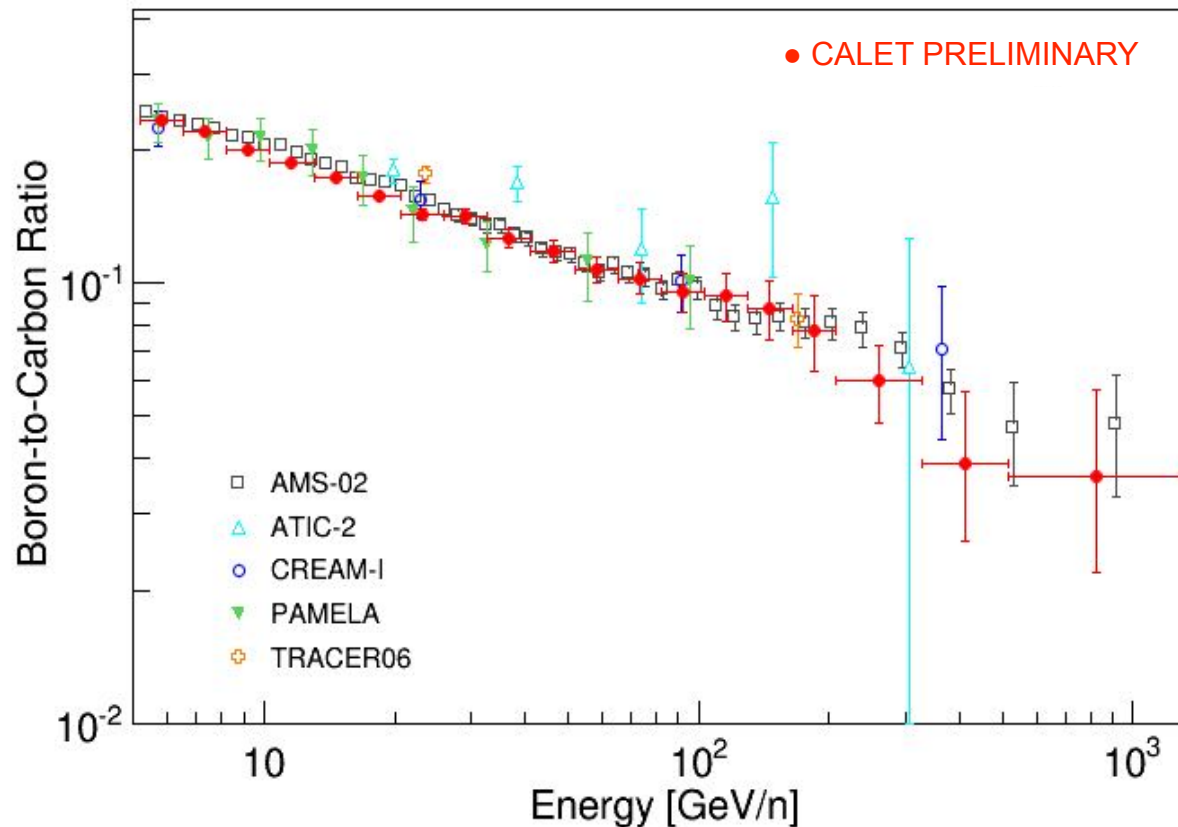


Note: there are no MC data above 100TeV for C, Ne Mg and Si.



# Preliminary Boron to Carbon Ratio in 20 GeV-1 TeV

Observed B/C vs energy per nucleon



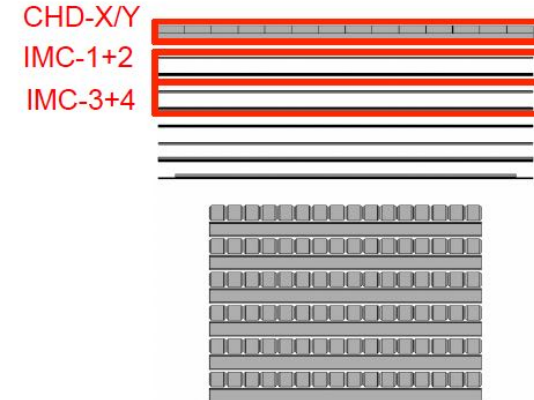
CALET preliminary results are consistent with recent AMS-02 with a power index of  $-1/3$ , as expected in the Kolmogorov turbulence regime, showing no clear saturation above 100 GeV/n as expected by a models assuming the existence of a constant residual material (grammage) during propagation.



# Preliminary Ultra Heavy Nuclei Measurements for $26 < Z \leq 40$

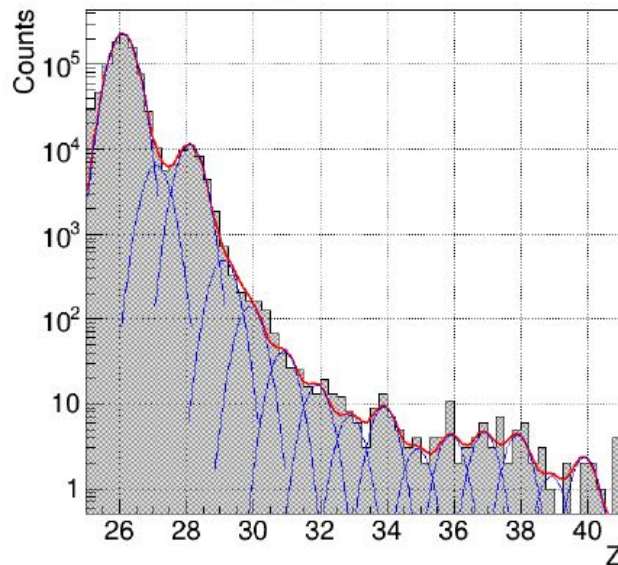
- CALET measures the relative abundances of ultra heavy nuclei through  ${}_{40}\text{Zr}$
  - Trigger for ultra heavy nuclei:
    - Signals of only CHD, IMC1+2 and IMC3+4 are required
    - an expanded geometrical acceptance ( $4000 \text{ cm}^2\text{sr}$ )
    - Energy threshold depends on the geomagnetic cutoff rigidity
- Data analysis

Onboard trigger for UH events

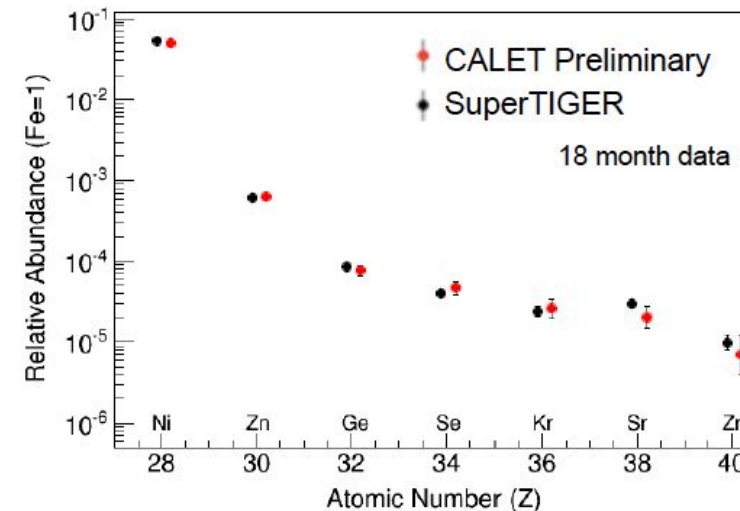


- Event Selection: Vertical cutoff rigidity  $> 4\text{GV}$  & Zenith Angle  $< 60$  degrees
- Contamination from neighboring charge are determined by multiple-Gaussian function

Charge distribution



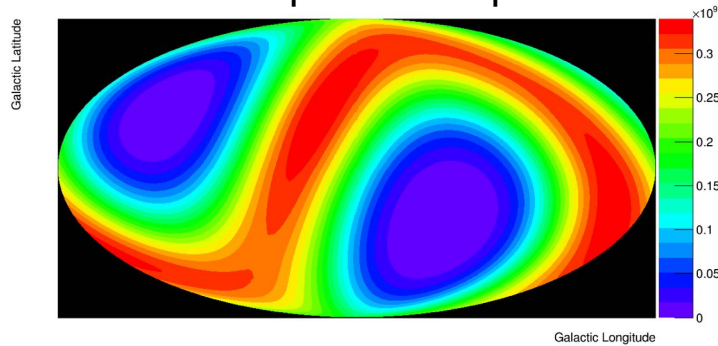
Relative abundance (Fe=1)





# CALET $\gamma$ -ray Sky in LE ( $>1\text{GeV}$ ) Trigger

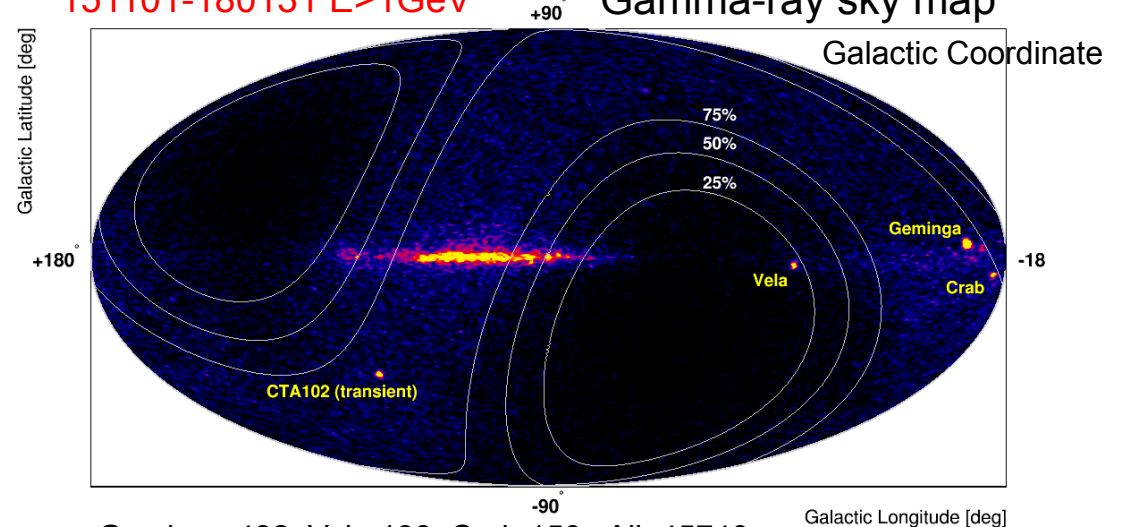
Exposure map



Exposure is limited to low latitude regions  
 $\Rightarrow$   $|\text{declination}| > 60 \text{ deg}$  is hardly seen  
 in LE gamma-ray trigger mode.

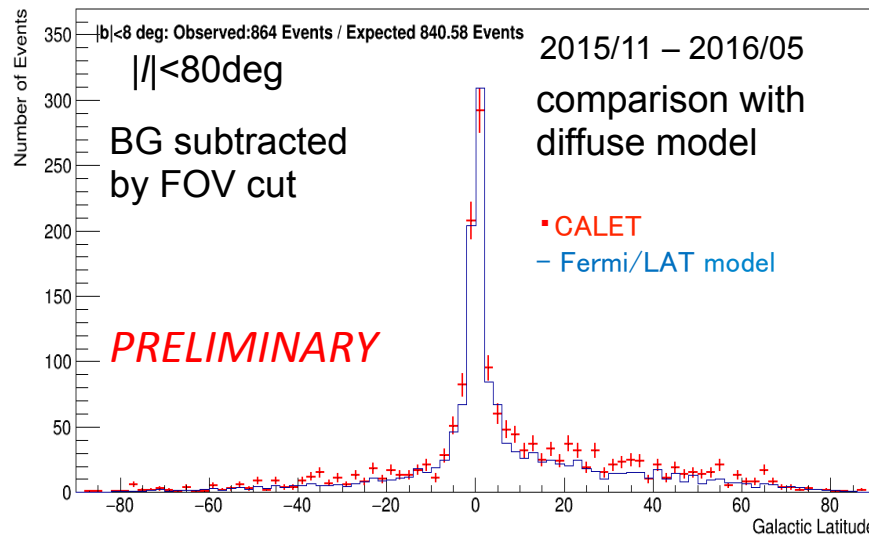
151101-180131  $E > 1\text{GeV}$

Gamma-ray sky map

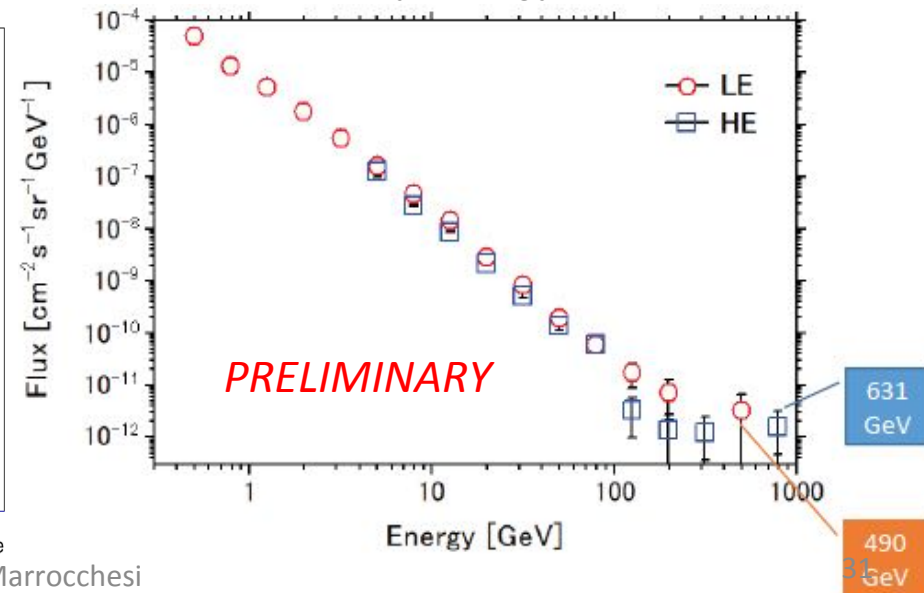


Geminga:432 Vela:138 Crab:150 All: 45740

Galactic diffuse gamma-rays



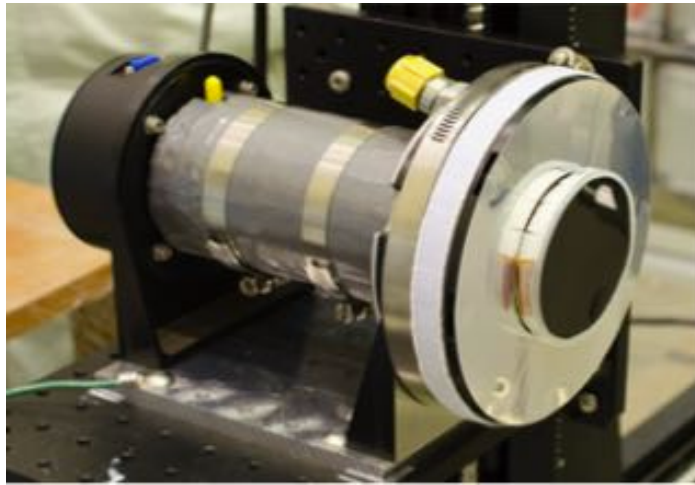
Gamma-ray energy spectrum





# CALET Gamma-ray Burst Monitor (CGBM)

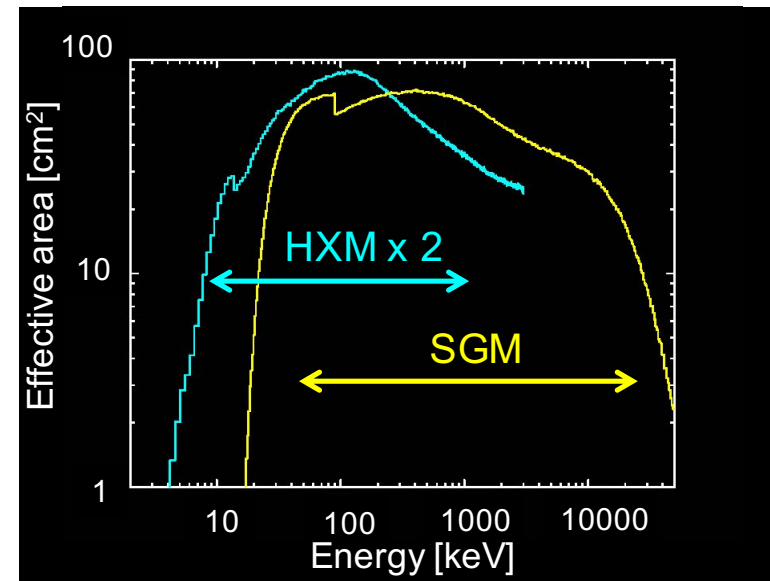
## Hard X-ray Monitor (HXM)



## Soft Gamma-ray Monitor (SGM)



	HXM (x2)	SGM
Detector (Crystal)	LaBr <sub>3</sub> (Ce)	BGO
Number of detector	2	1
Diameter [mm]	61	102
Thickness [mm]	12.7	76
Energy range [keV]	7-1000	100-20000
Energy resolution@662 keV	~3%	~15%
Field of view	~3 sr	~2π sr







# Summary of gamma-ray burst observations

## CGBM Operation Status

- Scientific observation: **October 6, 2015**
- Observation efficiency: **~60%** (HV-on time)
- **On-board trigger alert** (GCN notice)  
([http://gcn.gsfc.nasa.gov/calet\\_triggers.html](http://gcn.gsfc.nasa.gov/calet_triggers.html))

## CGBM GRB Statistics

(As of Sep 30, 2017)

- **74 GRBs** (only confirmed GRBs)
- GRB rate: **~37 GRBs/yr**
- 63 long GRBs (**85%**), 11 short GRBs (**15%**)  
c.f., Fermi-GBM: 82% long GRBs, 18% short GRBs (Paciesas et al. 2012)
- 49 spectroscopic GRB samples

- The time-averaged spectral parameters of CGBM are consistent with those of BATSE, Swift/BAT and Fermi-GBM.

# CALET UPPER LIMITS ON X-RAY AND GAMMA-RAY COUNTERPARTS OF GW 151226

Astrophysical Journal Letters 829:L20(5pp), 2016 September 20

The CGBM covered 32.5% and 49.1% of the GW 151226 sky localization probability in the 7 keV - 1 MeV and 40 keV - 20 MeV bands respectively. We place a 90% upper limit of  $2 \times 10^{-7}$  erg cm<sup>-2</sup> s<sup>-1</sup> in the 1 - 100 GeV band where CAL reaches 15% of the integrated LIGO probability ( $\sim 1.1$  sr). The CGBM 7  $\sigma$  upper limits are  $1.0 \times 10^{-6}$  erg cm<sup>-2</sup> s<sup>-1</sup> (7-500 keV) and  $1.8 \times 10^{-6}$  erg cm<sup>-2</sup> s<sup>-1</sup> (50-1000 keV) for one second exposure. Those upper limits correspond to the luminosity of  $3\text{-}5 \times 10^{49}$  erg s<sup>-1</sup> which is significantly lower than typical short GRBs.

CGBM light curve at the moment of the GW151226 event

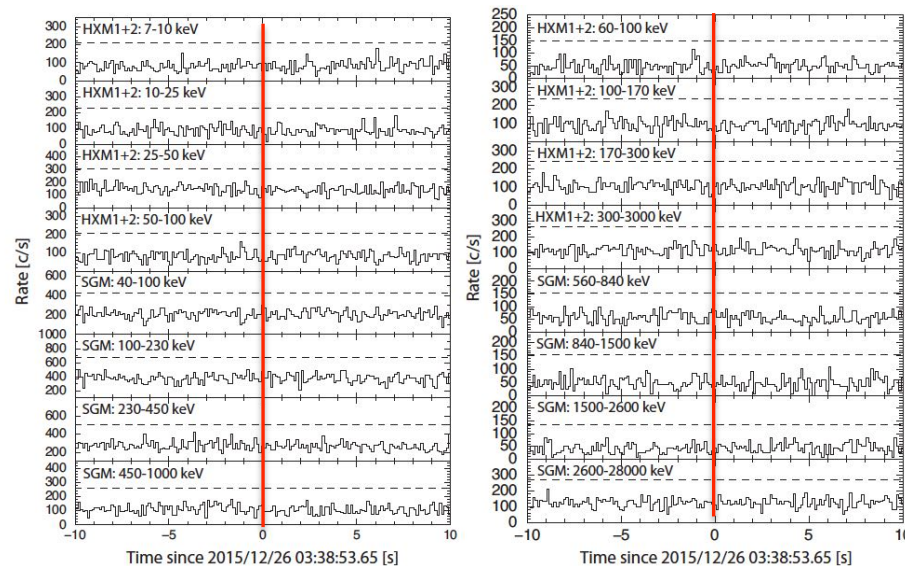


Figure 1. The CGBM light curves in 0.125 s time resolution for the high-gain data (left) and the low-gain data (right). The time is offset from the LIGO trigger time of GW 151226. The dashed-lines correspond to the 5  $\sigma$  level from the mean count rate using the data of  $\pm 10$  s.

Upper limit for gamma-ray burst monitors and Calorimeter

HXM: 7-500 keV

SGM: 50-1000 keV

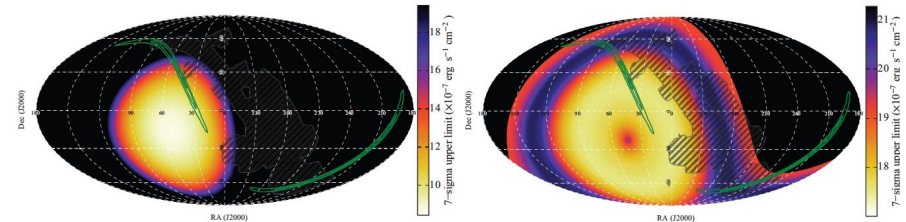


Figure 2. The sky maps of the 7  $\sigma$  upper limit for HXM (left) and SGM (right). The assumed spectrum for estimating the upper limit is a typical BATSE S-GRBs (see text for details). The energy bands are 7-500 keV for HXM and 50-1000 keV for SGM. The GW 151226 probability map is shown in green contours. The shadow of ISS is shown in black hatches.

Calorimeter: 1-100 GeV

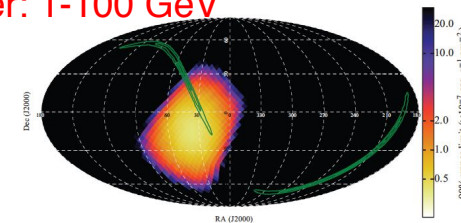


Figure 3. The sky map of the 90% upper limit for CAL in the 1-100 GeV band. A power-law model with a photon index of  $-1$  is used to calculate the upper limit. The GW 151226 probability map is shown in green contours.

# CALET's first publication was NOT for Cosmic Rays

Accepted article online 25 APR 2016

## Geophysical Research Letters

### Relativistic electron precipitation at International Space Station: Space weather monitoring by Calorimetric Electron Telescope

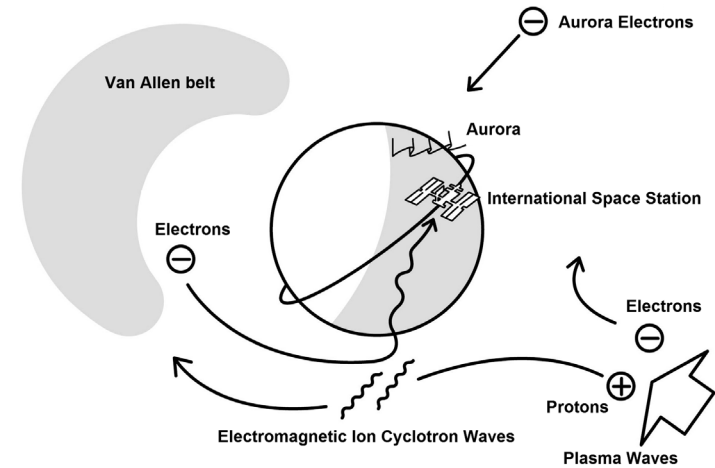
Ryuhō Kataoka<sup>1,2</sup>, Yoichi Asaoka<sup>3</sup>, Shoji Torii<sup>3,4</sup>, Toshio Terasawa<sup>5</sup>, Shunsuke Ozawa<sup>4</sup>, Tadahisa Tamura<sup>6</sup>, Yuki Shimizu<sup>6</sup>, Yosui Akaike<sup>4</sup>, and Masaki Mori<sup>7</sup>

<sup>1</sup>Space and Upper Atmospheric Sciences Group, National Institute of Polar Research, Tachikawa, Japan, <sup>2</sup>Department of Polar Science, School of Multidisciplinary Sciences, SOKENDAI (Graduate University for Advanced Studies), Tachikawa, Japan, <sup>3</sup>Research Institute for Science and Engineering, Waseda University, Shinjuku, Japan, <sup>4</sup>Department of Physics, Waseda University, Shinjuku, Japan, <sup>5</sup>Institute for Cosmic Ray Research, University of Tokyo, Kashiwa, Japan, <sup>6</sup>Institute of Physics, Kanagawa University, Yokohama, Japan, <sup>7</sup>Department of Physical Sciences, Ritsumeikan University, Kusatsu, Japan

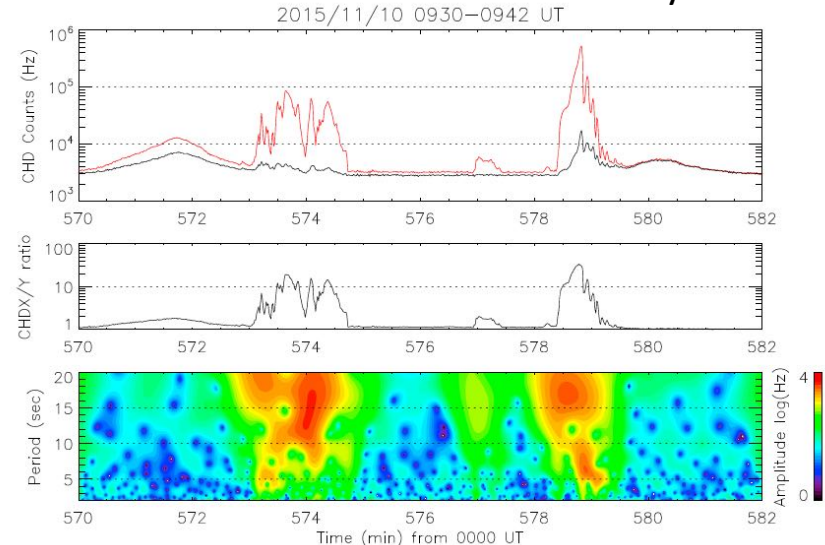
**Abstract** The charge detector (CHD) of the Calorimetric Electron Telescope (CALET) on board the International Space Station (ISS) has a huge geometric factor for detecting MeV electrons and is sensitive to relativistic electron precipitation (REP) events. During the first 4 months, CALET CHD observed REP events mainly at the dusk to midnight sector near the plasmapause, where the trapped radiation belt electrons can be efficiently scattered by electromagnetic ion cyclotron (EMIC) waves. Here we show that interesting 5–20 s periodicity regularly exists during the REP events at ISS, which is useful to diagnose the wave-particle interactions associated with the nonlinear wave growth of EMIC-triggered emissions.

Space Weather is now a new topic of CALET observations !

### Relativistic Electron Precipitation



### CHD X and Y count rate increase by REP





# Summary and Future Prospects

- ❑ CALET was successfully launched on Aug. 19th, 2015. The observation campaign started on Oct. 13th, 2015. Excellent performance and remarkable stability of the instrument.
- ❑ As of Feb. 28, 2018, total observation time is 870 days with live time fraction to total time close to 85 %. Nearly 570 million events collected with high energy (>10 GeV) trigger.
- ❑ Accurate calibrations have been performed with non-interacting p & He events + linearity in the energy measurements established up to  $10^6$  MIP.
- ❑ Preliminary analysis of nuclei, electrons (+ positrons) and gamma-rays have successfully been carried out and spectra obtained in the energy range:  
proton: 50 GeV~100 TeV, helium: 10 GeV-20 TeV/n, C-Fe: 300 GeV~100 TeV,  
B/C ratio: 20 GeV/n-1TeV/n, All electrons: 10 GeV~4.5 TeV.
- ❑ Preliminary analysis of UH cosmic rays up to Z=40.
- ❑ CALET's CGBM detected 74 GRBs in the energy range 7 keV-20 MeV. Follow-up observations of the GW events were carried out.
- ❑ The so far excellent performance of CALET and the outstanding quality of the data suggest that a 5-year observation period is likely to provide a wealth of new interesting results.